Primate Biol., 2, 25–56, 2015
www.primate-biol.net/2/25/2015/
doi:10.5194/pb-2-25-2015

Primate Biology
Open Access

Early development of the nervous system of the eutherian *Tupaia belangeri*

W. Knabe and S. Washausen

Prosektur Anatomie, Westfälische Wilhelms-Universität, 48149 Münster, Germany

Correspondence to: W. Knabe (w.knabe@uni-muenster.de)

Received: 16 April 2015 – Revised: 11 May 2015 – Accepted: 12 May 2015 – Published: 16 June 2015

Abstract. The longstanding debate on the taxonomic status of *Tupaia belangeri* (Tupaiidae, Scandentia, Mammalia) has persisted in times of molecular biology and genetics. But way beyond that *Tupaia belangeri* has turned out to be a valuable and widely accepted animal model for studies in neurobiology, stress research, and virology, among other topics. It is thus a privilege to have the opportunity to provide an overview on selected aspects of neural development and neuroanatomy in *Tupaia belangeri* on the occasion of this special issue dedicated to Hans-Jürg Kuhn. Firstly, emphasis will be given to the optic system. We report rather "unconventional" findings on the morphogenesis of photoreceptor cells, and on the presence of capillary-contacting neurons in the tree shrew retina. Thereafter, network formation among directionally selective retinal neurons and optic chiasm development are discussed. We then address the main and accessory olfactory systems, the terminal nerve, the pituitary gland, and the cerebellum of *Tupaia belangeri*. Finally, we demonstrate how innovative 3-D reconstruction techniques helped to decipher and interpret so-far-undescribed, strictly spatiotemporally regulated waves of apoptosis and proliferation which pass through the early developing forebrain and eyes, midbrain and hindbrain, and through the panplacodal primordium which gives rise to all ectodermal placodes. Based on examples, this paper additionally wants to show how findings gained from the reported projects have influenced current neuroembryological and, at least partly, medical research.

1 Introduction

Deciphering structure–function relationships was and still is a central issue of anatomical research. In the field of modern embryology tremendous efforts have been made to decode the cellular and molecular mechanisms underlying key processes in the development of vertebrates. Using ever-more-sophisticated methods, the preponderant implementation of this type of research has brought about a plethora of fascinating insights. However, in a countermove, multi-species analyses were abandoned in favor of studies with just a few thoroughly examined organisms for reasons of content and, of course, also for economic reasons. This communication provides both a brief description of the neurodevelopmental and neuroanatomical projects which have been carried out by the groups of Hans-Jürg Kuhn and his former students using *Tupaia belangeri* (Tupaiidae, Scandentia, Euarchontoglires, Eutheria, Theria, Mammalia) as a model system, and an overview on how findings gained from these projects have influenced current neuroembryological and medical research.

Hans-Jürg Kuhn, in whose honor this special issue of *Primate Biology* is published, has authored, supervised, and inspired basic embryological writings to characterize "his" Tupaia model. On the other hand, Kuhn has provided ideally and materially a long-term basis for future embryological research projects, mainly by building a comprehensive collection of histological series made from precisely staged paraffin- or resin-embedded embryos of *Tupaia belangeri*. This collection is managed by the Senckenberg Research Institute Frankfurt/Main, but housed in the *Prosektur Anatomie* of the Westfälische Wilhelms-Universität Münster, where it is of benefit for research projects of the group of Wolfgang Knabe which evolved from the former department of *Morphologie* (Georg-August-Universität, Göttingen) led by Hans-Jürg Kuhn.

Published by Copernicus Publications on behalf of the Deutsches Primatenzentrum GmbH (DPZ).

At the beginning of our Tupaia project, comparative anatomical studies were performed worldwide and in large numbers. Consequently, the phylogenetic position of *Tupaia belangeri* was under discussion in Göttingen and elsewhere – and still remains a matter of debate. Thus, after inclusion of molecular and genetic analyses the exact degree of relationship among the orders Primates, Dermoptera, and Scandentia within the superordinal group Euarchonta is still unclear (Janečka et al., 2007; Nie et al., 2008), and examination of the mitochondrial DNA even suggests a closer relationship between Scandentia and Lagomorpha (Schmitz et al., 2000; Arnason et al., 2002), which, in combination with rodents, have a sister-group relationship to Euarchonta.

Given the pragmatic value and the "transience" of biological classifications, Kuhn recognized *Tupaia belangeri* standing "at the roots of Primates". He accepted the preliminary taxonomic status of tree shrews as a separate order (Scandentia) and, already in Frankfurt, started to collect as many embryos and nest young *Tupaia belangeri* as possible (Kuhn and Starck, 1966). After the optimization of the breeding conditions for *Tupaia belangeri* in captivity (Schwaier, 1973, 1974), an extensive investigation on the implantation, early placentation, and the chronology of embryogenesis in *Tupaia belangeri* was published by Kuhn and Schwaier (1973) using embryos from 10 different stages of development, which came from the anatomical institute (Kuhn and Starck, 1966) and, mainly, from the former Battelle Institute in Frankfurt (Fig. 1). However, entirely in line with the already implied unwillingness to enter the arena of overhasty conclusions, Kuhn and Schwaier (1973) stated that "more information must be collected from nonspecialized mammals, the so-called Insectivora, Strepsirhini, and others, before all these characteristics and the pattern of reproductive biology of Tupaia can be included in the discussion of the systematic position of the Tupaiidae. It is most important that exactly dated embryos from animals bred under controlled conditions become available for future studies".

Both objectives were successfully fulfilled in Göttingen, where Kuhn managed to establish a close, long-term cooperation between the anatomical institute and the newly founded German Primate Center. During this period, basic embryological data were predominantly published in the framework of doctoral theses, and they covered five main topics:

1. the reproductive system (ovary: Kriesell, 1977; fallopian tube: Köpsel, 1988; fertilization and cleavage: Herrmann, 1982; postpartum erythrophagocytosis, iron storage, and iron secretion in the endometrium: Zeller and Kuhn, 1994),

2. the cardiovascular system (venous system of the liver: Liebherr, 1983; heart and epicardium: Kuhn and Liebherr, 1987, 1988; Schönemann, 1990; Otte, 1991; sinus venosus: Maas, 1992; anterior cardinal vein and its tributaries: Steinecker, 1989; arteries of the visceral arches: E. Dawid, 1989; posterior cardinal vein: Klammler, 1990; arteries of the upper extremity: Matsumoto et al., 1994; arteries of the lower extremity: Funke, 1995; Funke and Kuhn, 1998),

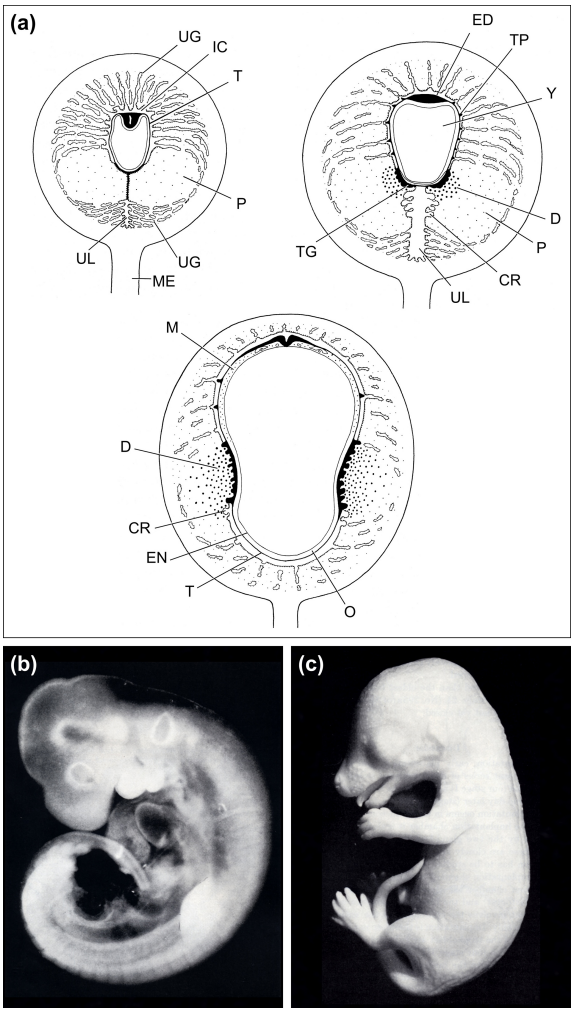

Figure 1. Implantation and embryonic development of *Tupaia belangeri*. **(a)** At embryonic day (E) 7 (primordial amniotic cavity stage, top left scheme), the blastocyst resides in the implantation chamber (IC) and is initially attached to the antimesometrial (ME, mesometrium) surface of the two apposed endometrial pads (P). At the embryonic disc (ED) stage (E9, top right scheme), the implantation chamber opens. The now-separated endometrial pads exhibit endometrial crypts (CR) on the mesometrial half of their surfaces. At the neural groove stage (E9, lower scheme), the blastocyst is completely attached to the surface of the endometrial pads. The omphalopleure (O) contacts the mesometrial pole of the uterine lumen. D, decidua; EN, endoderm; M, mesenchyme; T, trophoblast; TP, trophoblast plugs; UG, uterine glands; UL, uterine lumen; Y, yolk sac. **(b)** E14, total length: 4.14 mm. **(c)** E29, total length: 24 mm. Reproduced from Kuhn and Schwaier (1973, Figs. 10, 13, 14).

3. the skull (dentition: Jerxsen, 1982; cranium: Zeller, 1983; primary lateral wall of the skull: Bischoff, 1989),

4. the postcranial skeleton (Schumann, 1984; shoulder girdle: Eickhoff, 1989; chorda dorsalis: B. Dawid, 1989; skeleton of the foot: Ernstberger, 1994, with U. Zeller),

5. the nervous system (ontogenesis of the neocortex: Rehkämper, 1977; pituitary gland: Blanck, 1983; retina: Kühne, 1983; Knabe, 1995).

In the mid-1990s, the embryological research focus of our department increasingly shifted to the development of the nervous system of *Tupaia belangeri*, and here specifically to the development of the visual system. There are numerous anatomical features which make *Tupaia belangeri* highly suitable for studies on the visual system (e.g., Zilles, 1978). Consequently, around 200 scientific contributions on this subject have been published since 1966, dealing with structure–function relationships of the visual cortex, superior colliculi, lateral geniculate nuclei, pulvinar, optic tract, optic chiasm, suprachiasmatic nucleus, accessory optic system, retina, dioptric apparatus, and sclera.

2 Visual system

2.1 "Lens mitochondria" in the cone inner segments

In contrast to many other mammals, the entire retina of *Tupaia belangeri* mainly contains cones, whereas the number of rods amounts to only around 4 % on average (Samorajski et al., 1966; Kühne, 1983; Immel and Fisher, 1985; Foelix et al., 1987). Different from photoreceptor cells in mice and men, the nuclei of these cones are not stacked upon one another, but clearly arranged in only one row. Consequently, both the development of cones and rods (Knabe, 1995; Knabe and Kuhn, 1996a, b, 1997, 1998a; Knabe et al., 1997) and the establishment of the associated neural networks can be studied under particularly favorable conditions (Müller and Peichl, 1991a, b; Engelmann and Peichl, 1996; Sandmann et al., 1997; Knabe et al., 2007). On the other hand, the tree shrew retina is consulted in clinical contexts due to its extensive structural similarity to the primate retina, e.g., for documentation of retinal thinnings following induced high myopia via in vivo optical coherence tomography (Abbott et al., 2009, 2011).

Retinal cones of *Tupaia belangeri* demonstrate a further amazing structural feature. In their inner segments – which, in the optical path, are situated immediately before the light-perceiving cone outer segments – reside extraordinarily large mitochondria with "unique patterns of concentric cristae arranged in highly ordered whorls of lamellar configurations" (Samorajski et al., 1966; Dieterich, 1968, 1969; Kühne, 1983; Foelix et al., 1987). According to Foelix et al. (1987) these large mitochondria are formed by fusion of many smaller ones.

Building on this state of the art, we have extensively investigated the morphogenesis of megamitochondria in the retinal cones of *Tupaia belangeri* using 3-D reconstruction techniques (Knabe, 1995; Knabe and Kuhn, 1996a). It turned out that initially small, structurally unspecialized, and randomly distributed mitochondria migrate into the developing inner segment, thereby exhibiting a basal-to-apical size gradient which later is overlaid by a radial size gradient. Furthermore, all megamitochondria are constructed according to a basic building plan (Fig. 2a, b). They demonstrate a voluminous body situated in the center of the inner segment. From these bodies protrude long-drawn-out processes which run underneath the cell membrane and apparently give off small mitochondria. In the absence of clear proof of mitochondrial fusion, differential growth processes of individual mitochondria should contribute to the morphogenesis of these megamitochondria.

In the cone inner segments of *Tupaia belangeri*, long-drawn-out processes of megamitochondria and their presumed small derivatives are particularly suited to serve metabolic functions: first, due to their surface-to-volume ratio and, second, due to their proximity to the cell membrane. However, for these same reasons, an exclusive metabolic function of the voluminous, centrally located bodies of these megamitochondria seemed unlikely. Instead, we felt reminded of the "oil droplets" or "ellipsosomes" which, albeit of unknown origin, are situated in identical positions in the cone inner segments of teleosts, amphibians, reptiles, birds, and aplacental mammals (for a review, see Knabe and Kuhn, 1996a). Resembling mitochondria, ellipsosomes are ensheathed by a double membrane and may enclose rather diffuse membranous structures (Berger, 1966; Ishikawa and Yamada, 1969; Kunz and Regan, 1973; Kunz and Wise, 1978; for a review, see MacNichol Jr. et al., 1978). In contrast, classical oil droplets are bounded by a single membrane, demonstrate a completely homogeneous inner structure, and contain high quantities of carotenoids (Ishikawa and Yamada, 1969; Hailman, 1976; Borwein, 1981). A clear dividing line between ellipsosomes and oil droplets does not exist. However, it is widely accepted that usually colored oil droplets have a high index of refraction, may direct light towards the outer segment, and/or may filter out at least some wavelengths of the spectrum (Wolbarsht, 1976). In the light of these earlier results, our findings in *Tupaia belangeri* favor the hypothesis that huge specialized organelles with accessory optical functions have evolved from inner segment mitochondria in representatives from all vertebrate classes, thereby exhibiting a variety of different structural patterns ranging from "true" megamitochondria to highly modified oil droplets (Knabe and Kuhn, 1996a).

In the cone inner segments of *Tupaia belangeri* the cristae of megamitochondria are organized in the form of multilamellar wavelike crista-matrix systems (Fig. 2c) which are longitudinally oriented towards the outer segment and which, even between different individuals, demonstrate iden-

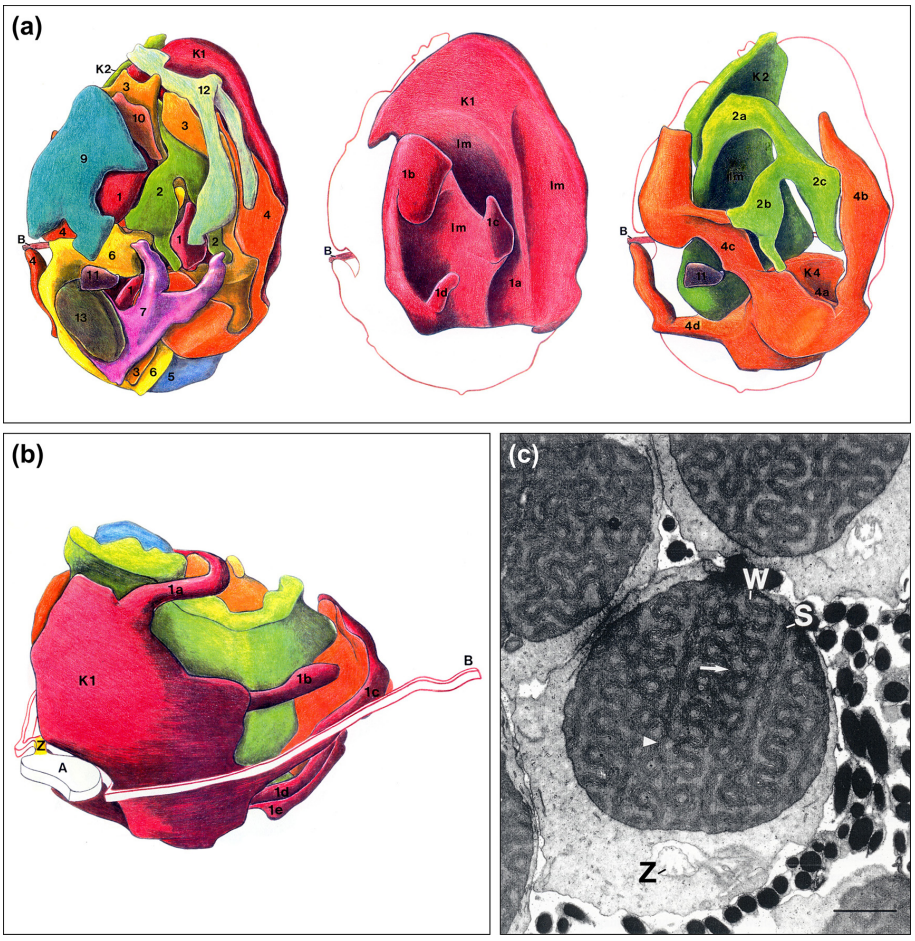

Figure 2. Morphogenesis of megamitochondria in retinal cone inner segments of *Tupaia belangeri*. **(a)** 3-D reconstructions, 12-day-old Tupaia: mitochondria (individually numbered and color-coded) are distributed in a basal (B)-to-apical size gradient. Megamitochondria (1, 2, and 4) exhibit voluminous apical bodies (K) and slender basal processes (a–d). Im, impressions from neighboring mitochondria. **(b)** 3-D reconstruction of apical megamitochondria which, in the cone inner segment of a 17-day-old Tupaia, are more subtly arranged in a basal-to-apical size gradient. Again, voluminous apical bodies (K1) and long-drawn-out basal processes (1a–1e) are discernible. A, cone outer segment; Z, cilium. **(c)** Transmission electron micrograph, 20-month-old Tupaia. Groups of four or five cristae pervade the apicalmost megamitochondrion either in a wavy (W) or in a straight (S) pattern. Note the switch of patterns within individual groups (arrowhead) and presumed junctions between adjacent groups (arrow). Scale bar = 1 µm. Reproduced from Knabe (1995, Figs. 17, 18, 19, 26, 35). © the author 1995.

tical "frequencies", "wavelengths", and "amplitudes" (Knabe, 1995; Knabe et al., 1997). In view of this high degree of order, we decided to determine the refractive index of isolated cone inner segments in cooperation with Sergej Skatchkov (Laboratory of Neurobiology, University of Puerto Rico, San Juan, Puerto Rico). It turned out that cone inner segments of *Tupaia belangeri* have higher refractive indices than the cone inner segments of all other mammals investigated so far ($X_A = 1.405$), which nicely fits our postulate that huge "lens mitochondria" may execute accessory optical functions (Knabe et al., 1997). Precise knowledge of the refractive indices and of the geometry of photoreceptor cells are required to further analyze the question how exactly waveguide theories can be applied to photoreceptor cells (McIntyre and Pask, 2013).

Reported characteristics of the retinal cones of *Tupaia belangeri* were quickly integrated in the canon of retinological knowledge (Ahnelt and Kolb, 2000) and have inspired quite numerous follow-up studies. It turned out that, contrary to some expectations, the structural composition of the inner segment mitochondria found in *Tupaia belangeri* is by no means the complete exception compared with other mammals. Instead, megamitochondria with presumed accessory optical functions were also discovered in the cone inner segments of several species belonging to the genus Sorex (Insectivora, Soricidae). As is also the case in *Tupaia belangeri*, these megamitochondria (1) are situated in apical and central

positions of the inner segment, whereas additional small mitochondria reside in its basal and peripheral parts; (2) possess an electron-dense matrix and a complex system of cristae; and (3) demonstrate cristae displaying a "continuous array from one large mitochondrion to several neighboring ones" (Lluch et al., 2003, 2009). An equivalent to megamitochondria also appears to exist in nocturnal *Microcebus murinus* (gray mouse lemur), which are the most ancestral living primates. Dkhissi-Benyahya et al. (2001) argue that "for the nocturnal mouse lemur, a gain in the sensitivity of cones could be useful during periods of dawn and dusk when light levels are in the low photopic range".

The presence of megamitochondria in photoreceptor cells is not restricted to mammals. Instead, megamitochondria also have been found in zebrafish, namely in the inner segments of cones as well as rods (Kim et al., 2005). Going beyond this initial characterization, Tarboush et al. (2012, 2014) have focused on the development of megamitochondria in zebrafish photoreceptor cells. Furthermore, these authors have assigned individual characteristics of the inner segment mitochondria to each of the four different types of cones as well as to rods. So far, similar efforts have not been successful in *Tupaia belangeri*, although two types of cones have been characterized spectroscopically (Petry and Hárosi, 1990) and immunocytochemically (Müller and Peichl, 1989). Staining with toluidine blue even revealed three subpopulations of cones, one of which is, however, unevenly distributed and, most probably, pathologically altered (Müller and Peichl, 1989). Using electron microscopy, Foelix et al. (1987) observed different electron densities in the mitochondrial matrix of cones which, however, were randomly distributed.

With regard to "accessory" functions of megamitochondria in the inner segments of zebrafish photoreceptor cells, Tarboush et al. (2014) primarily suggest mechanisms of protection against apoptotic processes, mainly due to the presence of crocetin, which reduces oxidative damage. Nevertheless, the authors think it possible that highly refractive photoreceptor cells of zebrafish act as light-funnelling devices, and they support our hypothesis that especially the small mitochondria underneath the cell membrane drive the energy metabolism (Tarboush et al., 2014).

In another teleost (*Fundulus heteroclitus*, killifish), the inner segments of photoreceptor cells do not contain megamitochondria in the proper sense, but instead a "variety of ellipsosome-like bodies" (Flamarique and Hárosi, 2000). Based on structural criteria, their descent from mitochondria is highly probable, whereas presumed accessory optical functions are currently a matter of speculation. According to Flamarique and Hárosi (2000), three different types of specialized organelles (electron-dense bodies, ellipsosomes, and pseudoellipsosomes with low optical density) are present in distal parts of the inner segments of long/middle-, long/long-wavelength double cones, or in single short-wavelength cones, respectively. Furthermore, these authors provide evidence for the first time that different types of ellipsosomes exist in photoreceptor cells taken from different parts of the retina.

"Large globules of mitochondrial origin" (ellipsosomes) with presumed accessory optical functions also have been observed in the Southern Hemisphere lamprey *Geotria australis* (Collin et al., 2003). This finding is particularly revealing from a phylogenetic perspective, since lampreys and hagfishes represent "the sole survivors of the very early agnathan (jawless) stage in vertebrate evolution" (Hardisty, 1982). Interestingly, in *Geotria australis*, ellipsosomes were exclusively found in medium-wavelength-sensitive cones of nocturnally active upstream migrants, but not in downstream migrants (Collin et al. 2003). Hence, ellipsosomes replace the yellow, short wavelength absorbing pigment present in downstream migrants and may help to trap photons.

Different from *Geotria australis*, not two types of cones but a single class of rod-like photoreceptors with cone-like features was documented in the Southern Hemisphere lamprey *Mordacia mordax* Richardson (Collin and Potter, 2000). Reminiscent of our findings in *Tupaia belangeri* (Knabe and Kuhn, 1996a), these rods contain "a large mitochondrial ellipsosome" on top of the inner segment mitochondria which are roughly lined up along a basal-to-apical size gradient. The ellipsosomes are dark without cristae, thus resembling the ellipsosomes of teleosts (Collin and Potter, 2000). Finally, oil droplets but not ellipsosomes are present in the cone inner segments of diurnal geckos, again on top of mitochondria arranged along a basal-to-apical size gradient (Röll, 2000).

As a prerequisite for designing experiments which clarify how exactly megamitochondria of the "Tupaia-type" influence the incoming light, the physical properties of their crista architecture need to be characterized in depth. Consequently, using the example of *Tupaia belangeri*, Almsherqi et al. (2012) dared to have a "look through 'lens' cubic mitochondria". The 3-D simulation data provided by them demonstrate that megamitochondria which contain multilayer cubic membrane structures may act as multifocal lenses, angle-independent interference filters to block UV-light, and/or waveguide photonic crystals. For a broader review on the properties of nanoperiodic cubic membranes see Almsherqi et al. (2009).

An understanding of how multi-layer cubic membrane structures contribute to the optic properties of megamitochondria will also help to characterize the optical properties of less spectacular inner segments exhibiting neither megamitochondria nor size gradients. In the simplest case, varying the number of mitochondria in different photoreceptor cell types and/or in different retinal positions may be sufficient to adjust the guidance of light to particular requirements. In line with this hypothesis, peripheral cones in *Macaca arctoides* contain excess mitochondria which possibly "enhance their light-gathering properties". Furthermore, the number of mitochondria is 10 times higher in cones compared to rods (Hoang et al., 2002).

Addressing the optical properties of photoreceptor cells which, by geometry of the outer segment alone, "compensate for self-screening of the visual pigments" and/or for a "signal-to-noise ratio decline along the longitudinal dimension" (Hárosi and Novales Flamarique, 2012) will remain a fascinating research objective. Introducing megamitochondria into this field as a new mosaic piece has inspired the search for other organelles which are placed in the optic pathway and which may have an influence on the incoming light. Thus, it recently became clear that the rod nuclei of nocturnal animals – unlike the "conventional" rod nuclei of diurnal species – demonstrate a centrally located condensation of heterochromatin. Due to the resulting increase of the refractive index, such "inverted" rod nuclei may in fact "act as collecting lenses" (Solovei et al., 2009). In this regard, exciting observations also have been published by Joffe et al. (2014), who are interested in how diurnality has developed in Primates. Based on the analysis of proteins responsible for the marginalization of heterochromatin in rod nuclei, it turned out that primate ancestors were nocturnal and that "transition to diurnality occurred independently in several primate and related groups" including Tupaia. From the authors' point of view, the "hemispherical lens formed by a giant mitochondrion" in the cone inner segments of Tupaia represents an extreme adaptation to diurnality and, thus, predestines *Tupaia belangeri* for follow-up studies on this problem. Correspondingly, Joffe et al. (2014) demonstrate that, in the cones of *Tupaia belangeri*, nucleoli with high refractive indices are constantly situated at the inner pole of the cone nucleus and may act as a "second lens".

Irrespective of the question to which extent megamitochondria in the cone inner segments of *Tupaia belangeri* provide energy equivalents and/or assist in guiding light, mitochondria are relevant for studies in age research. This holds especially true for megamitochondria which facilitate refined investigations of the mitochondrial DNA (Primmer, 2002), all the more so as the complete mitochondrial genome of *Tupaia belangeri* has already been analyzed (Schmitz et al., 2000). In the context of age research, other advantages of tree shrews, compared with rodents, are their longevity and their phylogenetic status closer to humans (Primmer, 2002).

2.2 Ciliogenesis in photoreceptor cells

Having completed our 3-D reconstructions of cone inner segments, we next wanted to learn more about the mechanisms which regulate the highly ordered immigration of mitochondria into the developing cone inner segments of *Tupaia belangeri*. We discovered contacts between migrating mitochondria and groups of microtubules originating from the pair of centrioles which is situated in apicalmost parts of the inner segments. Obviously, these microtubules serve as a guide for mitochondria (Fig. 3a, Knabe and Kuhn, 1996b). Only thereafter does the "connecting cilium" spring from the apical centriole of the microtubule-organizing center (MTOC) and transform into the light-absorbing outer segment (Knabe and Kuhn, 1997, 1998a).

So far, a microtubule apparatus which supports the migration of mitochondria into the developing cone inner segment has not been demonstrated in any other vertebrate. Nevertheless, similar arrangements of microtubules exist during the redistribution of mitochondria in developing Müller cells of the rabbit retina (Germer et al., 1998). However, the observed pattern of microtubules does not permit full-length guidance, and oxygen gradients may play the major role in this context. For another example, a structure resembling the Drosophila fusome which is involved in anchoring centrioles and organizing the primary mitochondrial cloud around the centriole was found during female germline cyst development in *Xenopus laevis* (Kloc et al., 2004). Mitochondria also appear to be moved by microtubules during merozoite assembly in *Plasmodium falciparum* (Hopkins et al., 1999), and mitochondrial dysfunction results from abnormal microtubules in cytoplasmic male sterility of higher plants (Li et al., 2014, in conjunction with findings of Zhang et al., 2009).

In the cones of *Tupaia belangeri*, onset of ciliogenesis precedes the outgrowth of the inner segment by about half the gestation time. Up to 1 week after birth, the two centrioles responsible for ciliogenesis are situated centrally and, thus, reside in an ideal position to support the immigration of mitochondria into the developing inner segment (Fig. 3a). Only after this do the two centrioles as well as the associated connecting cilium shift from central to excentric positions (Figs. 2c, 3a) and, most astonishingly, in hundreds of neighboring cones to one and the same side of the inner segment (Knabe and Kuhn, 1997). Studies of this type help to improve our understanding (1) of protein sorting, targeting and trafficking in photoreceptor cells (Pearring et al., 2013); (2) of the procedures and meaning underlying the apical positioning of primary cilia (Kong et al., 2013; Wheway et al., 2014); and (3) of general aspects of ciliogenesis and cilium-based diseases (Insinna and Besharse, 2008; Gakovic et al., 2011). However, our major discovery in this context remains the coordinated relocation of the connecting cilium to identical excentric positions (Knabe and Kuhn, 1997), which also takes place in zebrafish (Ramsey and Perkins, 2013). In the adult zebrafish, cilia are situated asymmetrically on the cell edge nearest to the optic nerve in red-, green-, and blue-sensitive cones, but not in ultraviolet-sensitive cones or rods. Thus, motile as well as immotile cilia demonstrate patterns of planar polarity (Ramsey and Perkins, 2013). However, it is still unclear how this type of planar polarity is established in cones and what its functional impacts are. This may be about to change in view of the exciting new discovery that, in kidney epithelial cells, primary cilia ($9 + 0$ cilia) undergo active fluctuations in the absence of dyneins (Battle et al., 2015).

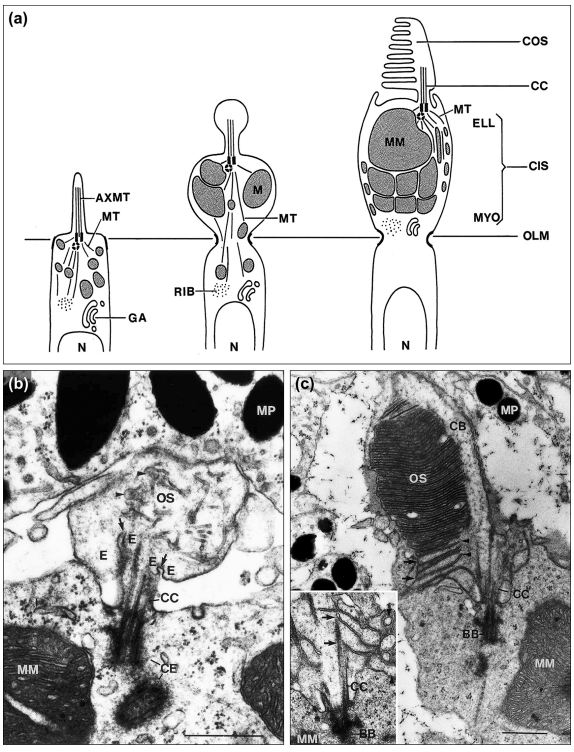

Figure 3. Development of retinal cones in *Tupaia belangeri*. **(a)** Inner segment mitochondria. Embryonic day 32 (left scheme): small supranuclear mitochondria are attached to cytoplasmic microtubules (MT). The primitive cilium (AXMT, axonemal microtubules) projects beyond the outer limiting membrane (OLM). 12-day-old Tupaia (middle scheme): the developing inner segment extends beyond the OLM. MTs originate from centrally located centrioles and guide individually growing mitochondria into the inner segment. In the adult (right scheme), all inner segment mitochondria including megamitochondria (MM) reside in the ellipsoid (ELL). The connecting cilium (CC) links the cone outer segment (COS) to the cone inner segment (CIS). Note that centrioles and CC are shifting from central to excentric positions. GA, Golgi apparatus; MYO, myoid; N, nuclei; RIB, ribosomes. **(b–c)** Disk formation, transmission electron micrographs (longitudinal sections). In the 12-day-old Tupaia **(b)**, evaginations (E) of the plasma membrane have formed at the base of the immature outer segment (OS) that contains tubulovesicular material (arrowhead). Next to the connecting cilium (CC), the membranes of adjacent evaginations are joined in the initial disk rims (arrows). CE, centrioles; MP, melanin granules. In the 17-day-old Tupaia **(c)**, plenty of nearly mature disks are aligned at the ciliary backbone (CB) of the outer segment. Note initial disk rims (arrowheads) as well as evaginations (arrows) of the plasma membrane that project from the inner face of the cilium. Inset: obliquely sectioned basal outer segment: "the initial disk rims are hooked (arrows) to the axonemal microtubules". BB, basal body of the connecting cilium. Scale bars = 0.5 µm. Figure 3a is reproduced from Knabe and Kuhn (1996b), Fig. 5, by permission of John Wiley & Sons, Inc. Fig. 3b, c is reproduced from Knabe and Kuhn (1998, Figs. 2, 4). © Springer-Verlag 1998, with kind permission from Springer Science and Business Media.

2.3 Cone outer segments

In the (for now) last ultrastructural work our group has published on the development of photoreceptor cells, focus was given to the formation of disks in the cone outer segments (Knabe and Kuhn, 1998a, also for review). Morphogenesis of the membranous disks which contain the visual pigments has been explained differently so far. According to the first hypothesis, disks arise from vesicles which pinch off from the basal cell membrane of the outer segment and then fuse and flatten (Obata and Usukura, 1992; Usukura and Obata, 1995). In this model, continuity between the interior of the disks and the extracellular space, as seen in mature cones, results from the secondary fusion between the disks and the cell membrane of the outer segment. In contrast, disks in the developing cone outer segments of *Tupaia belangeri* develop between the apposed membranes of two neighboring "basal evaginations" (Steinberg et al., 1980; Eckmiller 1987, 1990) rich in cytoplasm, which protrude from the position of the eccentrically localized ciliary axoneme to the opposite side (Fig. 3b, c). Consequently, from the very beginning, the interior of newly formed disks opens to the extracellular space. The reservation must be made that, in both scenarios, the interior of the disks represents incorporated extracellular space. The only difference seems to be a heterochrony of the formation of the disks and their internalization. Later, Holcman and Korenbrot (2004) demonstrated that different patterns of disk formation in cones and rods, the latter finally revealing disks not joined with the plasma membrane, are responsible for the different diffusion characteristics of the excitation signal cGMP in cones and rods, respectively.

2.4 Horizontal cells

Another project looked at whether retinal neurons, with the exception of neurovascular contact points serving vasoregulation, are completely separated from the basal lamina of capillaries by macroglial cells (astrocytes and Müller cells). Using a combination of transmission electron microscopy, immunohistochemistry, and lectin histochemistry, the structural links between endothelial cells, pericytes, glial cells, and neurons were studied in the four vascular layers of the retina of adult *Tupaia belangeri*. Much to our surprise, an incomplete macroglial ensheathment of the capillaries was observed, most notably in the outer capillary layers 1 and 2 (Fig. 4). In capillary layer 1, which is located between the inner nuclear layer and the outer plexiform layer, these "gaps" were filled with the perikarya and electron-lucent processes of horizontal cells that, in single sections, ensheathed up to approximately 9 / 10 of the capillary circumference (Knabe and Ochs, 1999). We therefore postulated that "current concepts of retinal function and pathology, which are based on the assumption that retinal vessels are strictly isolated from retinal neurons, at least in *Tupaia*, might deserve reconsideration".

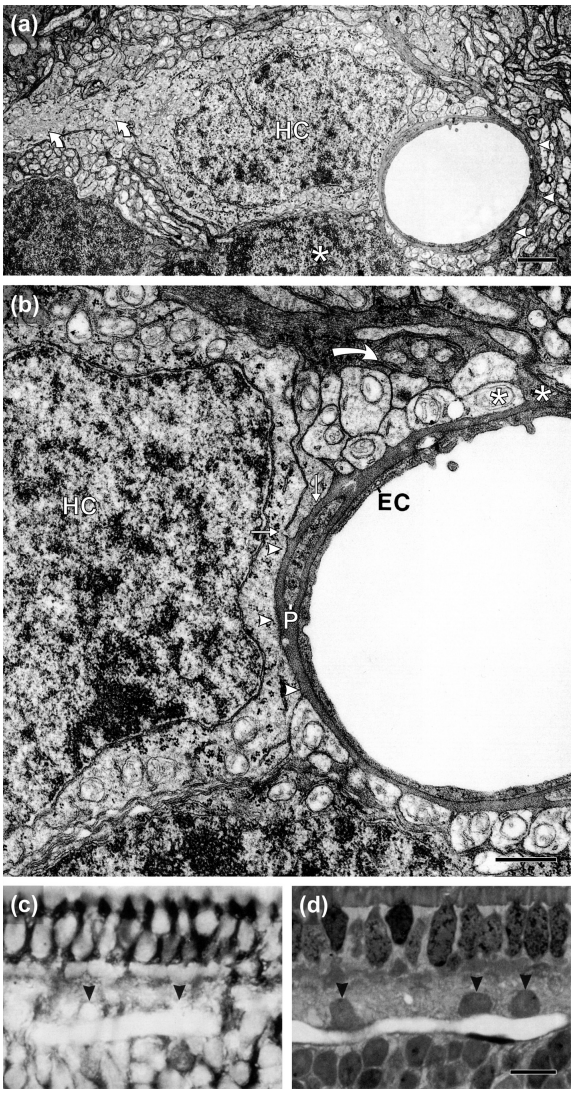

Figure 4. Horizontal cells ensheath capillaries in retinal capillary layer 1, adult *Tupaia belangeri*. **(a, b)** Transmission electron micrographs. **(a)** A horizontal cell (HC) invests the basal lamina of the capillary that, on the opposite side, is ensheathed by electron-dense processes of Müller cells (white arrowheads). Curved arrows, horizontal cell dendrite; asterisk, bipolar cell nucleus. **(b)** Detailed view of **(a)**. The electron-lucent perikaryon of the horizontal cell contacts the capillary basal lamina (arrowheads). Electron-lucent processes of the horizontal cell (continuity with the perikaryon indicated by small arrows) are enclosed by the electron-dense processes of Müller cells (curved arrow; asterisks: alternating contacts of electron-dense and electron-lucent processes at the capillary basal lamina). EC, endothelial cell; P, process of a pericyte. **(c)** The S-100-immunopositive glial ensheathment of the capillary is interrupted by horizontal cell perikarya (arrowheads). For a comparison, see **(d)**: section thickness 1 µm, hematoxylin. Scale bars = 1 µm in **(a)**; 0.5 µm in **(b)**; 10 µm in **(c, d)**. Reproduced from Knabe and Ochs (1999, Figs. 1, 6a, b). © Springer-Verlag 1999, with kind permission from Springer Science and Business Media.

To define the scope of our findings more accurately, in a second step, an unbiased stereological method was used to determine the extent of basal lamina occupied by macroglial Müller cells and non-macroglial cells, respectively, in the three outer capillary layers of the central retina of adult *Tupaia belangeri* (Ochs et al., 2000). It turned out that the mean (standard deviation) percentage surface coverage by non-Müller cell processes was 46.8 (15.3) % (layer 1), 3.0 (2.1) % (layer 2), and 0.3 (0.3) % (layer 3). In most cases, capillary-contacting non-Müller cells in capillary layer 1 belonged to horizontal cells of the mammalian type A (Knabe and Kuhn, 2000).

Based on immunohistochemical and confocal microscopic techniques, extensive vascular contacts of retinal horizontal cells proved to be present also in rats and mice and, thus, "appear to be a more common theme for these neurons than previously appreciated" (Mojumder, 2008). Equally important are efforts to decipher the functions as well as the possible pathological consequences of the vascular contacts of horizontal cells. On the assumption that retinal cilia are capable of detecting potentially harmful changes in the extracellular environment, Kim et al. (2013) have studied the presence of cilia in the retina of adult mice. It could be shown that ciliary markers (Arl13b, a small GTPase localized on cilia membrane; acetylated alpha-tubulin; adenyl cyclase III) are expressed, among other places, by the processes of horizontal cells which, due to their extensive neurovascular contacts (Knabe and Ochs, 1999; Mojumder, 2008), are predestined for monitoring and controlling the extracellular milieu.

Pathological situations in which vascular contacts of horizontal cells play a role have been demonstrated in mice with oxygen-induced retinopathy, where links appear to exist between neurovascular cell injury and the arginase pathway (Suwanpradid et al., 2014). Beforehand, Ahuja et al. (2005) aimed to clarify whether and how glutathione S transferase (GST) helps to protect photoreceptor cells. Using rd1/rd1 mice containing an insertion of viral DNA in the β-subunit of the cGMP phosphodiesterase gene, reduced amounts of α- and µ-GST were found in Müller cell end feet as well as in large caliber horizontal cell fibers. Consequently, Ahuja et al. (2005) speculated that, in wild-type mice, secreted GST may protect the retina against toxic molecules penetrating through the capillaries and invading the adjacent tissue. Alternatively, GST released from Müller cells and/or horizontal cells may interact with reduced glutathion and proteins adhering to the surface of photoreceptor cells and, thus, may help to bring about their survival. Also of particular interest are the research contributions made by Park et al. (2003a), who have studied the patterns of apoptotic death among photoreceptor cells in streptozotocin-induced diabetic rat retina. These authors demonstrate degenerative changes of horizontal cell processes already after 1 week, and this, most probably, happened thanks to their extensive vascular contacts, which make them "sensitive to any minute alteration in the capillaries".

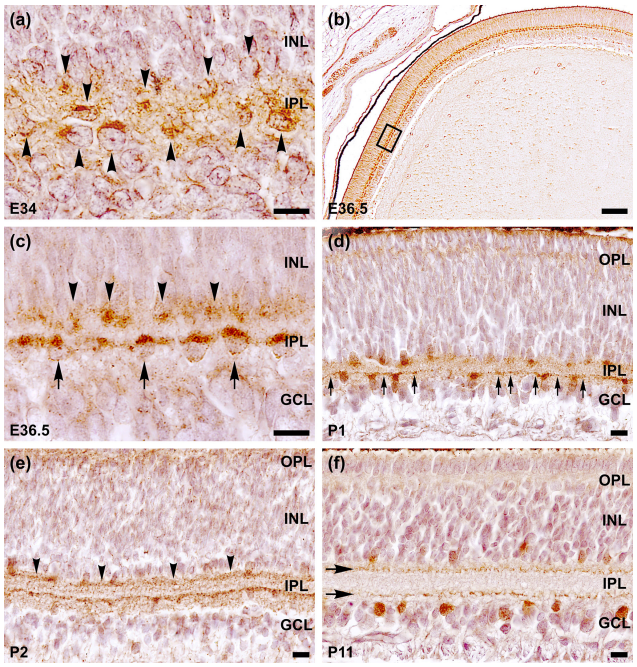

Figure 5. Development of starburst amacrine cells in the retina of *Tupaia belangeri*. **(a)** Appearance of anti-choline acetyltransferase (ChAT)-immunopositive precursors (arrowheads) in the developing inner plexiform layer (IPL) on embryonic day (E) 34. (**b**, **c**: detail magnified from boxed area in **b**) Segregation of orthotopic (arrowheads in **c**) and displaced starburst amacrines (arrows in **c**) on E36.5. **(d)** Prior to orthotopic amacrines, displaced amacrines start building up their dendritic band (arrows) already on postnatal day (P) 1. **(e)** Onset of stratification of orthotopic amacrines (arrowheads) on P2. **(f)** Two starburst amacrine cell strata are present on P11. GCL, ganglion cell layer; INL, inner nuclear layer; OPL, outer plexiform layer. Scale bars = 10 µm in **(a, c–f)**; 100 µm in **(b)**. Reproduced from Knabe et al. (2007, Fig. 2.) © 2007 Wiley-Liss, Inc., by permission of John Wiley & Sons, Inc.

Given the presumed impact of neurovascular contacts of horizontal cells on health and disease, it is actually staggering how little we know about the development of these contacts. Such investigations are the more necessary since Bosco et al. (2005) have observed a coordinate developmental switch of the expression of aquaporin-4 (AQP4) and inwardly rectifying K^+ channels (Kir4.1) from horizontal cells to Müller cells in the retina of mice as soon as they can see for the very first time. Based on the premise that AQP4 and Kir4.1 help to clear extracellular K^+ and water from the synaptic layers, Bosco et al. (2005) suggest that differentiating horizontal cells "may contribute to early retinal homeostasis" and, possibly, "fulfill an archetypal glial function". Expectations are high as to how the observed switch in the expression patterns of AQP4 and Kir4.1 correlates with the development of the extensive vascular contacts of retinal horizontal cells.

2.5 "Starburst" amacrine cells

Next we have investigated the development of cholinergic amacrine cells in the retina of *Tupaia belangeri* (Knabe et al., 2007). Through the optimization of standard immunohistochemistry protocols, cholinergic amacrine cells which play key roles "in originating retinal directional selectivity and optokinetic eye movement" (Yoshida et al., 2001) could be detected 2 weeks earlier than had been reported previously (Sandmann et al., 1997). This helped to demonstrate that, in mammals, two mirror-imaged subpopulations of cholinergic amacrine cells are derived from a single population of precursor cells (Fig. 5). Furthermore, refined knowledge of the similarities and dissimilarities which characterize the development of "orthotopic" starburst amacrines in the inner nuclear layer and "intentionally displaced" starburst amacrines in the ganglion cell layer facilitates differential diagnosis of these regular subpopulations from erroneously migrating "misplaced" starburst amacrines (Pérez de Sevilla Müller et al., 2007; for a comprehensive review, see Famiglietti and Sundquist, 2010).

In the retinal inner plexiform layer of *Tupaia belangeri*, establishment of mirror-imaged directionally selective circuits is initiated by the dendrites of cholinergic amacrine cells. These dendrites provide the scaffold for the dendrites of directionally selective ganglion cells which contact starburst amacrines with a delay (Knabe et al., 2007). Most probably, proper development of these networks depends on the presence of stable neurofilaments resulting from the coexpression of neurofilament protein M (NF-M, 150 kDa) and α-internexin in the dendrites of starburst amacrines (Fig. 6). As soon as the earliest functional synapses have formed in the inner plexiform layer (Foelix et al., 1987), both the dendrites of starburst amacrine cells and the dendrites of directionally selective ganglion cells downregulate NF-M and/or α-internexin (Knabe et al., 2007). The obvious question to ask here is whether the transient coexpression of these two neurofilament proteins not only stabilizes the dendrites of starburst amacrines and ganglion cells but also somehow promotes their mutual recognition. In the long term we are aiming to clarify whether the expression of different combinations of neurofilament proteins in the retina has anything to do with the selective vulnerability of certain of the neuronal classes which, for example, has been observed during diabetic retinopathy (Park et al., 2003b; Gastinger et al., 2006; Kern and Barber, 2008).

The temporary occurrence of α-internexin during defined developmental periods, as seen in the retina of *Tupaia belangeri* (Knabe et al., 2007), suggests that α-internexin might play a role in neuroplasticity. Under this premise, Liu et al. (2013) have studied the expression patterns of α-internexin in neuronal lineages of the developing chick retina. It turned out that, at least in early phases of development, chick embryos demonstrate a much broader expression profile for α-internexin compared with *Tupaia belangeri*

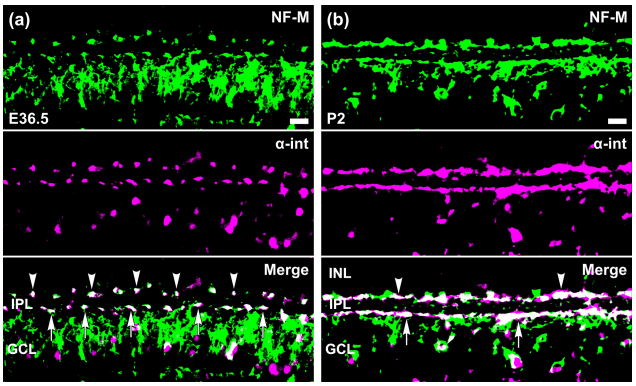

Figure 6. Development of starburst amacrine cells in the retina of *Tupaia belangeri*. Double-immunofluorescence with antibodies against medium-molecular-weight neurofilament (NF-M, green) and α-internexin (α-int, magenta). **(a)** Embryonic day 36.5: coexpression of NF-M and α-int in the supranuclear cytoplasm of orthotopic (arrowheads) and displaced starburst amacrines (arrows). **(b)** Postnatal day 2: coexpression of NF-M and α-int in the developing dendritic strata of orthotopic (arrowheads) and displaced starburst amacrines (arrows). GCL, ganglion cell layer; INL, inner nuclear layer; IPL, inner plexiform layer. Scale bars = 10 µm. Reproduced from Knabe et al. (2007, Fig. 6a, b). © 2007 Wiley-Liss, Inc., by permission of John Wiley & Sons, Inc.

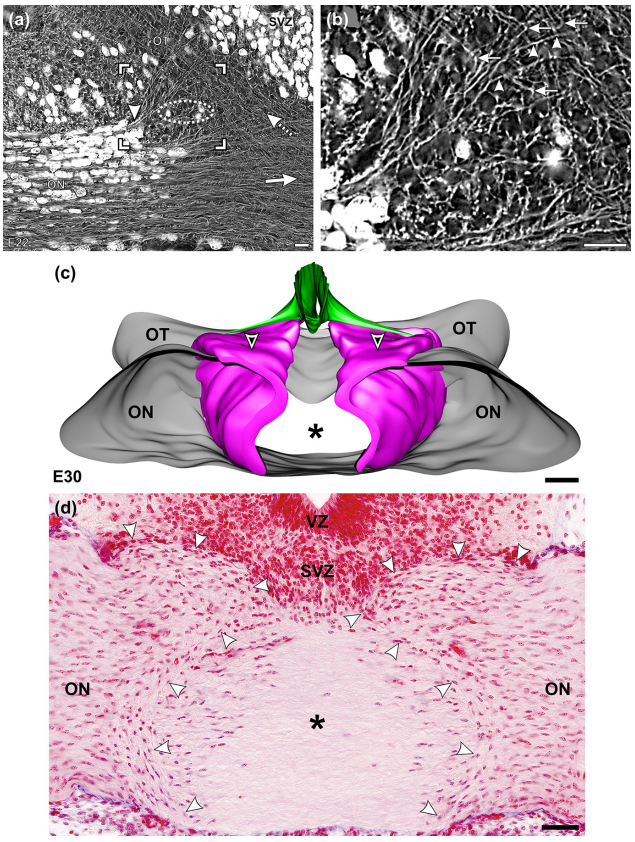

Figure 7. Glial arches deflect ipsilaterally projecting axons in the developing optic chiasm of *Tupaia belangeri*. **(a, b)** Embryonic day (E) 22: inverted gray-scale micrographs of a hematoxylin-eosin-stained horizontal section. **(a)** Leaving the optic nerve (ON), most axons project contralaterally (solid arrow), whereas ipsilaterally projecting axons (arrowhead) are deflected at the developing glial arch (dotted circle). Dotted arrow, crossing axons from the contralateral optic nerve; OT, optic tract; SVZ, subventricular zone. **(b)** Detail magnified from boxed area in **(a)**. Different from contralaterally projecting axons (arrowheads), ipsilaterally projecting axons are sharply deflected (arrows) lateral to the glial arch cell bodies. **(c)** E30: 3-D reconstruction. Glial arches (magenta) reside at the transition of the optic nerve and chiasm (gray). Green, SVZ of the third ventricle; arrowheads, position of the reconstructed Azan-stained coronal section shown in **(d)**, which demonstrates how cell bodies belonging to the glial arches "descend" (arrowheads) from the SVZ. Asterisk, chiasmatic midline; VZ, ventricular zone. Scale bars = 10 µm in **(a, b)**; 100 µm in **(c)**; 50 µm in **(d)**. Reproduced from Knabe et al. (2008, Figs. 4, 11). © 2008 Wiley-Liss, Inc., by permission of John Wiley & Sons, Inc.

(photoreceptor cells, horizontal cells, bipolar cells, amacrine cells, ganglion cells), whereas permanent expression is restricted to ganglion cells, amacrine cells, and horizontal cells. The functional meaning of interspecific differences regarding the physiological expression of α-internexin needs to be clarified in follow-up studies. Knowledge of these expression patterns is also relevant under pathological conditions, e.g., in a spontaneous equine model of autoimmune uveitis where vitreal IgM autoantibodies target NF-M in neuronal processes of the retina (Swadzba et al., 2012).

2.6 Optic chiasm

Whether the developing axons of retinal ganglion cells cross the chiasmatic midline or stay ipsilaterally depends, among other factors, on the interactions with "guide post cells". Studies on embryonic mice have revealed specialized radial glial cells as well as neurons of the anterobasal nucleus which express different sets of molecules capable of either repelling or attracting ganglion cell axons close to the brain midline (for reviews, see Williams et al., 2004; Jeffery and Erskine, 2005; Petros et al., 2008). Our observations on this point disprove the widely favored hypothesis that previous findings in mice are representative for all placental mammals. In the studied embryos of *Tupaia belangeri*, ipsilateral axons turn back towards their site of origin already in prechiasmatic parts of the optic nerve (Fig. 7a, b, Knabe et al., 2008; for adult Tupaia also see Jeffery et al., 1998), thus resembling marsupials (Taylor and Guillery, 1994; Harman and Jeffery, 1995; MacLaren, 1998). Consequently, it seemed to us rather improbable that axonal pathfinding in the optic chiasm of Tupaia should be primarily attributable to midline signalling. Actually, we noticed that the guidance of ipsilateral axons depends on "glial arches" (Fig. 7c, d) which are situated, bilaterally symmetrically, at the transition of the optic nerve to the optic chiasm and which originate from the lateral sub-

ventricular zones adjacent to the third ventricle (Knabe et al., 2008).

It turned out that, among placental mammals, segregation of ipsilaterally and contralaterally projecting axons by guide post cells at a distance from the chiasmatic midline, first reported in *Tupaia belangeri* (Knabe et al., 2008), is by far not the exception to the rule. Thus, Jeffery et al. (2008) postulated that a similar zone of decision-making should exist in *Callithrix jacchus*. The particular importance of the observations made in *Tupaia belangeri* (Knabe et al., 2008) and marmosets (Jeffery et al., 2008) lies in the fact that a similarly structured optic chiasm appears to exist in man. That also explains why, in man, developmental loss of one eye does not adversely affect the axonal projections of the remaining one – quite different from rodents where segregation of axons from both eyes depends on mutual interactions at the brain midline (Neveu et al., 2006). Accordingly, *Tupaia belangeri* (Knabe et al., 2008) and marmosets (Jeffery et al., 2008) are appropriate models for studying the mechanisms which regulate axonal pathfinding in the visual system of man.

3 Olfactory system

The joint research focus of Cordula Renate Malz, Hans-Jürg Kuhn, and colleagues was on the development of the olfactory systems of *Tupaia belangeri*. Additional studies were carried out on structure–function relationships in the pituitary gland and cerebellum.

3.1 Lectin binding

As a first step, Malz et al. (1999) investigated lectin-binding sites in the vomeronasal organ and in the olfactory epithelium. These findings support the hypothesis that specific sets of glycoproteins contribute to the histogenesis of the individual systems as well as to the recognition and transduction of olfactory/pheromonal stimuli. For example, alpha-N-acetylgalactosamine is expressed in the vomeronasal nerve but not in the olfactory nerve. Within the vomeronasal organ, alpha- and beta-N-acetyl-D-glucosamine are simultaneously present in the presumed regeneration zone. Finally, it appears possible that pregnancies have an influence on the abovementioned processes in the vomeronasal organ, as revealed by the different expression patterns of *Dolichos biflorus* lectin in pregnant and non-pregnant *Tupaia belangeri*.

Lectin panels provided by Malz et al. (1999) and others help to make a distinction between animals with functional or non-functional vomeronasal organs. Thus, markedly different overall patterns of lectin immunostaining were observed in vestigial vomeronasal organs of humans and chimpanzees compared with chemosensory vomeronasal organs in other primates (Kinzinger et al., 2005). Furthermore, knowledge of the lectin-binding patterns in the olfactory and nasal epithelia is a prerequisite for lectin-mediated DNA delivery during targeted mucosal immunization (Wang et al., 2005).

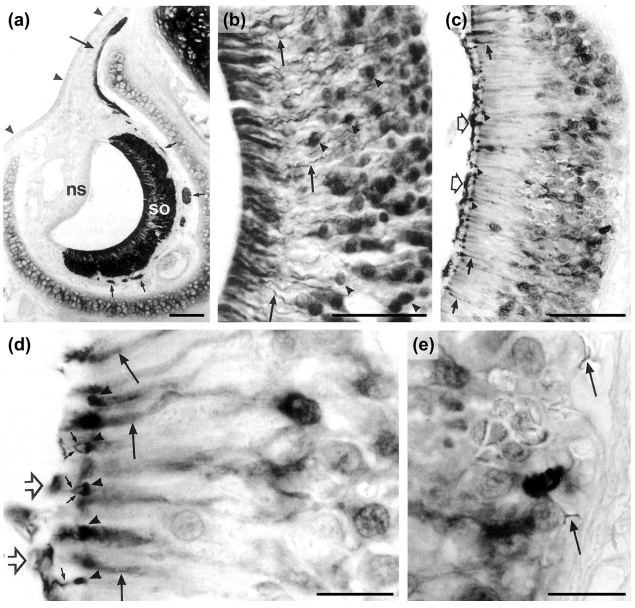

Figure 8. Calretinin immunoreactivity in the vomeronasal organ of adult *Tupaia belangeri*. **(a)** Immunoreactivity in the sensory epithelium (so), in vomeronasal nerve fiber bundles (small arrows), and in the vomeronasal nerve (large arrow). Arrowheads, respiratory epithelium; ns, non-sensory epithelium. **(b)** Immunopositive somata (arrowheads) and dendrites (arrows) of receptor cells. **(c)** Immunoreactivity in the mucus (open arrows), dendrites (solid arrows), and dendritic clubs (arrowheads) of receptor cells. **(d, e)** Enlarged from **(c)**. **(d)** Immunoreactivity in the mucus (open arrows), clumps of microvilli (small solid arrows), dendritic clubs (arrowheads), and dendrites (large solid arrows). **(e)** Immunopositive receptor cells and their axons (arrows). Scale bars = 150 µm in **(a)**; 50 µm in **(b, c)**; 15 µm in **(d, e)**. Reproduced from Malz et al. (2000, Fig. 5). © 2000 Wiley-Liss, Inc., by permission of John Wiley & Sons, Inc.

3.2 Calretinin

Thereafter, focus was placed on the expression patterns of calretinin, which belongs to the EF-hand family of calcium-binding proteins. According to Heizmann and Braun (1992) and Schwaller (2014), calretinin is involved in intracellular calcium signalling, mediates the calcium-buffering capacity of cells, and protects neurons against calcium overload. We aimed to clarify – for the first time extensively – whether different expression patterns of calretinin exist in the functionally different vomeronasal and main olfactory systems. It turned out that calretinin is present in virtually all vomeronasal receptor cells and fibers (Fig. 8), but only in subsets of receptor cells belonging to the main olfactory system (Malz et al., 2000). This means that only certain of the olfactory qualities are perceived under the influence of calretinin. Conversely, the number of calretinin-immunopositive interneurons was much higher in the main olfactory bulb compared with the accessory olfactory bulb (Fig. 9). Our observations further suggest that structurally and functionally

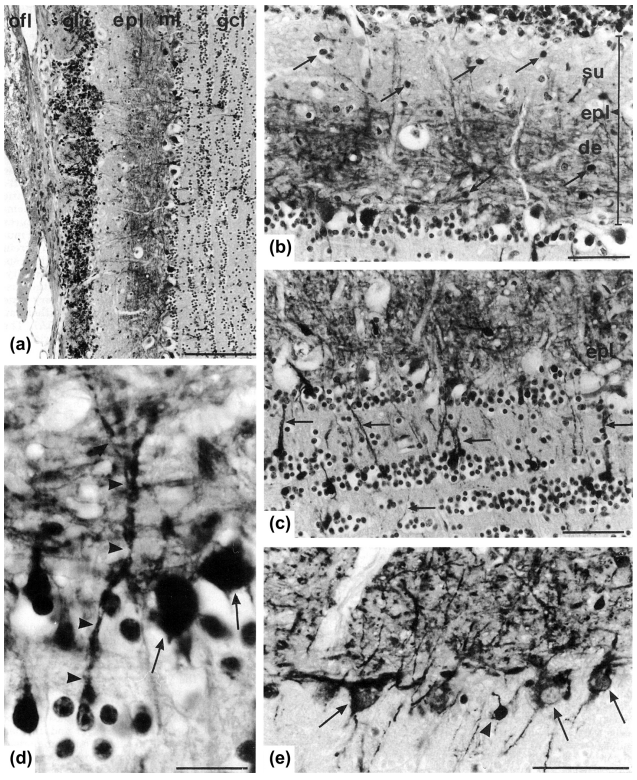

Figure 9. Calretinin immunoreactivity in the main olfactory bulb of adult *Tupaia belangeri*. **(a)** Overview: olfactory nerve fiber layer (ofl), glomerular layer (gl), external plexiform layer (epl), mitral cell layer (ml), and granular cell layer (gcl). **(b–e)** Detailed view of **(a)** rotated 90° clockwise. **(b)** Faint and strong immunoreactivity in the superficial (su) and deep (de) half of the epl, respectively. Arrows, immunopositive neuronal perikarya. **(c)** Immunoreactive granule cells and their processes (arrows). **(d)** Immunoreactivity in mitral cells (arrows) and in the dendrite of a granule cell (arrowheads). **(e)** Immunoreactivity in mitral cell somata (arrows) and processes as well as in an inner short axon cell (arrowhead). Scale bars = 150 µm in **(a)**; 50 µm in **(b, c, e)**; 15 µm in **(d)**. Reproduced from Malz et al. (2000, Fig. 3). © 2000 Wiley-Liss, Inc., by permission of John Wiley & Sons, Inc.

distinct subclasses of output cells (mitral cells, tufted cells) and interneurons help to establish a laminar organization of the external plexiform layer (EPL), which is subdivided into a weakly calretinin-immunopositive superficial layer and a strongly calretinin-immunoreactive deep layer (Malz et al., 2000). Correspondingly, Kakuta et al. (2001) demonstrated that, in insectivores (*Suncus murinus*) "the EPL is divided into the OSL [outer sublayer] and ISL [inner sublayer] based on the different meshworks of CB[calbindin]-positive neuronal processes (…), and based on the different densities of CR[calretinin]-positive fibers".

Our findings in *Tupaia belangeri* are required to clarify the interspecific variability of calretinin expression (Pombal et al., 2002: *Lampetra fluviatilis*; Castro et al., 2006: *Danio rerio*; Castro et al., 2008: *Salmo trutta fario*), and to facilitate comparison between the immunoreactive patterns of calretinin and other calcium-binding proteins (Jia and Halpern, 2003: calbindin-D28k, rat; Jia and Halpern, 2004: calbindin-D28k, parvalbumin, calretinin, *Monodelphis domestica*; Morona and González, 2008: calbindin-D28k, calretinin, anuran and urodele amphibians; Morona et al., 2011: calbindin-D28k, calretinin, *Dermophis mexicanus*; Kosaka and Kosaka, 2004: calbindin-D28k, rat, mouse, tree shrew, bat, hedgehog, laboratory musk shrew, mole). However, it must be pointed out that "the content of a particular calcium-binding protein in a neuronal group is not a fully reliable criterion for considering homologies" (Morona and González, 2008).

Knowledge of the expression patterns of calretinin and other calcium-binding proteins can be successfully applied for detecting the effects of gene mutations. Thus, as a consequence of lamination defects, an almost complete breakdown of the physiological expression pattern of calretinin was observed in the olfactory bulb of dlx5 (distal-less homeobox 5)$^{-/-}$ mice (Levi et al., 2003). Testing panels of calcium-binding proteins also facilitates functional studies of calcium-controlled processes, for example, in the frameworks of pulse stimulation of isolated olfactory neurons with odors and isobutylmethylxanthine/forskolin (Zhang and Delay, 2006) or following urine stimulation of the mouse vomeronasal organ, which activates large-conductance Ca^{2+}-activated K^+ channels (Zhang et al., 2008). Finally, a good understanding of the expression patterns of calcium-binding proteins helps to find answers to evolutionary biological problems, e.g., when analyzing the vomeronasal type 1 receptor (V1R) family (Young et al., 2010). One of the interesting results of this study is that "almost all of the species with large V1R repertoires have well-developed vomeronasal organs and/or AOBs [accessory olfactory bulbs]".

We subsequently investigated the expression patterns of calretinin and olfactory marker protein (OMP) in the developing vomeronasal and main olfactory systems of *Tupaia belangeri* (Malz et al., 2002). In the other mammals studied so far, calretinin expression levels start off very low at birth but then rapidly increase during postnatal development (Bastianelli et al., 1995; Kimura and Furukawa, 1998). Thus, it came to us as a surprise that, in *Tupaia belangeri*, strong expression of calretinin in receptor cells, nerve fibers, many interneurons, and projecting neurons of both olfactory systems was already present during embryonic development (Fig. 10). As a result, subpopulations of receptor cells of the vomeronasal system can now be distinguished prenatally by their profoundly differing degrees of calretinin expression (Malz et al., 2002).

Our findings in *Tupaia belangeri* have provided supplemental information for studies on the growth and maturational characteristics of the vomeronasal complex in nocturnal strepsirhines insofar as these are revealed by the expression pattern of OMP (Garrett et al., 2013). Similarly, Shimp et al. (2003) have investigated the ducts leading to

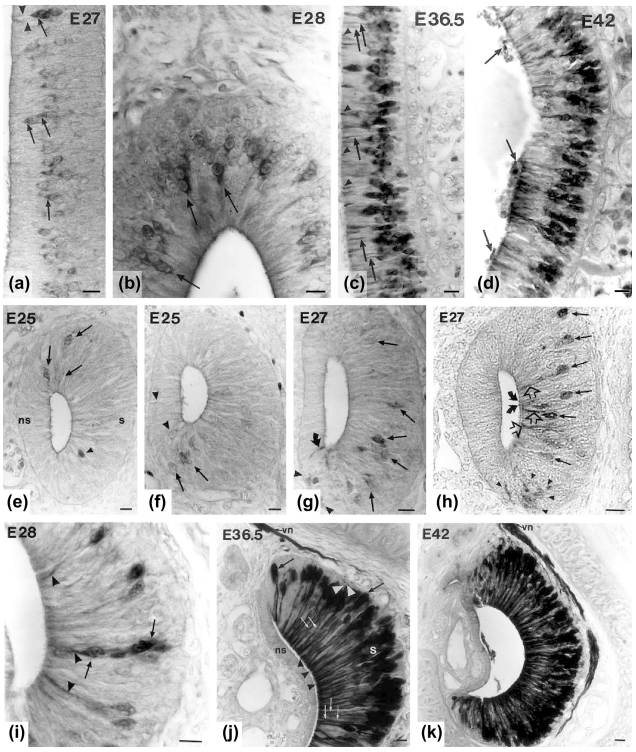

Figure 10. Calretinin immunoreactivity in the developing olfactory epithelium and vomeronasal organ of *Tupaia belangeri*. **(a–d)** Olfactory epithelium from embryonic day (E) 27 to 42. **(a)** E27: receptor cells (arrows), but not supporting cells (arrowheads) are immunopositive. **(b)** E28: strong immunoreactivity in the peri- and supranuclear cytoplasm (arrows) of receptor cells on E28. **(c)** E36.5: most receptor cells in the mid-zone are immunopositive. Arrows and arrowheads indicate their dendrites and terminal clubs, respectively. **(d)** E42: almost all receptor cells of the mid-zone express calretinin. Arrows, immunoreactivity in the superficial mucus. **(e–k)** Vomeronasal organ from E25 to E42. **(e)** E25: immunoreactive receptor cells in the sensory (s) epithelium (arrowhead) and in the transition zone to the non-sensory (ns) epithelium (arrows). **(f)** E25: weak immunoreactivity in presumed ectopic receptor cells in the non-sensory epithelium (arrowheads). Arrows, immunopositive receptor cells in the transition zone. **(g)** E27: the number of immunopositive receptor cells in the sensory epithelium (arrows) has increased. Arrowheads and curved arrows indicate weak immunoreactivity in basal cells and a presumed ectopic receptor cell, respectively. **(h)** E27: calretinin expression in clubs (curved arrows), dendrites (open arrows), and perikarya (arrows) of receptor cells. Arrowheads, immunopositive cell group at the transition zone. **(i)** E28: columnar formation (arrows) of immunopositive receptor cell perikarya. Arrowheads, receptor cell dendrites. **(j)** E36.5: immunoreactivity in clubs (arrowheads), dendrites (white arrows), perikarya (black arrows), and axons (white arrowheads) of receptor cells has increased. vn, vomeronasal nerve. **(k)** E42: calretinin expression in virtually all receptor cells and in the vomeronasal nerve. Scale bars = 10 µm in **(a–j)**; 20 µm in **(k)**. Reproduced from Malz et al. (2002, Figs. 2b–e, 7). © Springer-Verlag 2002, with kind permission from Springer Science and Business Media.

the vomeronasal organ in order to identify differences regarding the perinatal functionality of the vomeronasal system in primates (*Microcebus murinus*), mice, and insectivora. Compared with the data available for adult animals, much less is known about the expression patterns and functions of calcium-binding proteins in the developing olfactory systems (e.g., Halpern and Martínez-Marcos, 2003: mammals, VNO; Castro et al., 2008: *Salmo trutta fario*).

3.3 Terminal nerve

Malz and Kuhn (2002) have further demonstrated, for the first time in a placental mammal, the embryonic development of calretinin- and Phe-Met-Arg-Phe (FMRFamide)-immunoreactive neurons in the terminal nerve ("cranial nerve zero"; for a review, see Vilensky, 2014). This nerve is a "diffusely organized system of neurons" which emigrate from the olfactory placode and, in all jawed vertebrates, finally reside "within the nasal cavity and rostral forebrain" (Wirsig-Wiechmann et al., 2002). It runs in close vicinity to the main olfactory and vomeronasal nerves, contains compact ganglia, and also exists in humans (de Vries, 1905: cited in Larsell, 1950; Brookover, 1914; Johnston, 1914). Subpopulations of its neurons contain neuropeptides, among others gonadotropin-releasing hormone (GnRH), which modulate the activity of receptor cells (Wirsig-Wiechmann et al., 2002; Vilensky, 2014).

In *Tupaia belangeri*, calretinin and the cardioexcitatory tetrapeptide FMRFamide – the latter as early as GnRH – are expressed in different subpopulations of migrating and ganglionic neurons (Fig. 11, Malz and Kuhn, 2002). Later, Park et al. (2003a) demonstrated that, in *Ambystoma mexicanum*, FMRFamide dramatically increases the magnitude of a voltage-gated inward current in the olfactory receptor cells. In mouse olfactory sensory neurons, FMRFamide modulates potassium currents (Ni et al., 2008), whereas FMRFamide-like peptides exert inhibitory effects on the pacemaker activity of GnRH neurons in the freshwater tropical fish *Colisa lalia* (Saito et al., 2010). Other findings in *Tupaia belangeri* suggest that calretinin influences the migration and differentiation of neurons which are associated with the terminal nerve (Malz and Kuhn, 2002). In contrast, calretinin-immunoreactive migrating cells are absent from the terminal nerve in the brown trout (*Salmo trutta fario*; Castro et al., 2008).

Knowledge of the early pathways along which luteinizing hormone-releasing hormone (LHRH)- and FMRFamide-immunoreactive neurons reach the forebrain also helps in testing functional hypotheses. Thus, it turned out that, in newborn marsupials (*Macropus eugenii*), these pathways are usually too immature to support guidance to the pouch and nipple (Ashwell et al., 2008). Accordingly, at birth, the degree of maturity of these olfactory pathways is not high enough to allow olfaction-mediated behavior in platypus and echidnas, "two modern monotreme lineages that

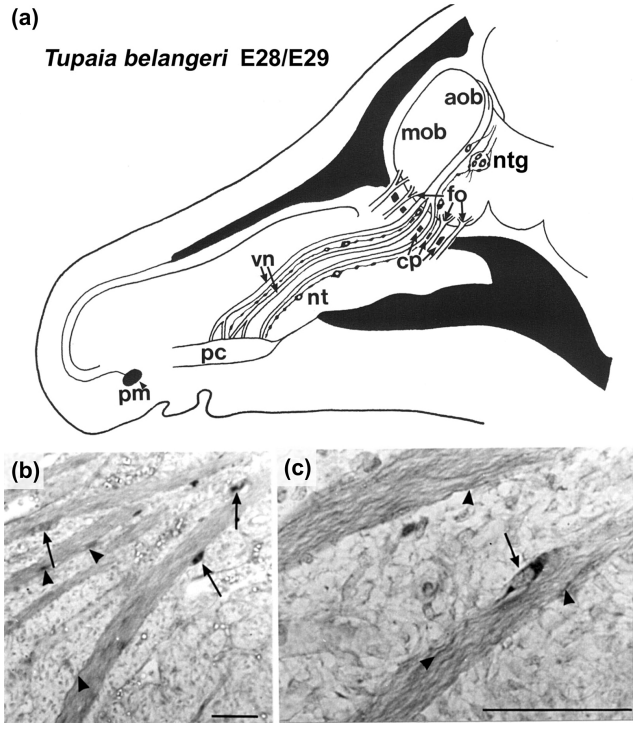

Figure 11. FMRFamide immunoreactivity in the developing terminal nerve of *Tupaia belangeri*. **(a)** Scheme of the vomeronasal system (right half of the head, nasal septum removed, embryonic day (E) 28/29). The vomeronasal organ is situated in the paraseptal cartilage (pc) and sends the vomeronasal nerve (vn) through the cribriform plate (cp) to the accessory olfactory bulb (aob). The main olfactory bulb (mob) is targeted by the fila olfactoria (fo). FMRFamide-immunopositive nervus terminalis neurons (nt) reside in the vomeronasal nerve and in the nervus terminalis ganglion (ntg). pm, premaxillary bone. **(b, c)** Immunopositive neurons (arrows) and nerve fibers (arrowheads) in the terminal nerve of E28 Tupaia. Scale bars = 50 µm. Reprinted from Malz and Kuhn (2002, Fig. 2). © 2002, with permission from Elsevier.

have followed independent evolutionary paths from a less olfaction-specialized ancestor" (Ashwell, 2012). Nevertheless, as in *Tupaia belangeri*, a terminal nerve including ganglia is present already prior to birth.

4 Pituitary gland

Based on the previous work by Blanck (1983), Malz and Kuhn (1999) have investigated whether invertebrate neuropeptides (in this case, FMRFamide) have counterparts in the pituitary gland of mammals. In the pituitary gland of *Tupaia belangeri*, FMRFamide is already present on embryonic day 27, and the adult labelling pattern is established around embryonic day 41. Overall, the findings of Malz and Kuhn (1999) indicate that FMRFamide contributes to the regulation of releasing factors as well as to the secretion of hormones. Furthermore, a subpopulation of FMRFamide-immunopositive cells is demonstrated which migrate from the pars intermedia to the neural lobe. Most probably, these cells represent invading basophils (Malz and Kuhn, 1999). Interestingly, a complex innervation pattern of FMRFamide-immunoreactive fibers was also found in the brain of *Salmo trutta fario* and, here, included moderate amounts of FMRFamide-labelled fibers in the pituitary gland (Castro et al., 2001).

5 Cerebellum

Parasagittal compartments in the cerebellar cortex with precisely regulated input and output characteristics are revealed by immunohistochemistry with antibodies against zebrin I (Hawkes and Leclerc, 1989). In cooperation with colleagues from the University of Calgary (Alberta, Canada) and the Riken Brain Science Institute in Wako-shi (Saitama, Japan), C. R. Malz has demonstrated that zebrin II (Brochu et al., 1990; epitope on the respiratory isoenzyme aldolase C: Ahn et al., 1994)-immunoreactive parasagittal stripes and transverse zones in the cerebellar cortex of *Tupaia belangeri* much more closely correspond to those of primates, compared with rodents or lagomorphs (Sillitoe et al., 2004). Confirmed by later findings in the laboratory mouse (Chung et al., 2008), zebrin-II-labelled compartments in *Tupaia belangeri* are not seen as all-or-none expression differences, but through differences in the intensity of immunostaining (Sillitoe et al., 2004).

Other groups have subsequently studied zebrin-II-immunoreactive cerebellar compartments in order to carry out the following investigations: (1) interspecific comparison with the tammar wallaby (*Macropus eugenii*) (Marzban et al. 2012), microchiropteran bats (Kim et al., 2009), hummingbirds (Aves: Trochilidae) (Iwaniuk et al., 2009), chicks (*Gallus domesticus*) (Marzban et al., 2010), pigeons (*Columba livia*) (Pakan et al., 2007; for an overview, see Marzban and Hawkes, 2011); (2) visualization of aldolase C with fluorescence through gene manipulation with the help of aldolase C-Venus knock-in mice to facilitate studies on cerebellar compartmentalization (Fujita et al., 2014); (3) presentation of parasagittal stripes in the vermis which, complementary to zebrin II, are immunoreactive for neurofilament H (Demilly et al., 2011); (4) identification of links between the olivocerebellar projection and zebrin-immunoreactive compartments in the laboratory mouse (Sugihara and Quy, 2007) and in marmoset (*Callithrix jacchus*) (Fujita et al., 2010); (5) clarification of the role played by the helix-loop-helix (HLH) transcription factor early B-cell factor 2 (EBF2) (Croci et al., 2006); and (6) evaluation of the cerebellar connectivity in spinocerebellar ataxia type 1 (Solodkin et al., 2011).

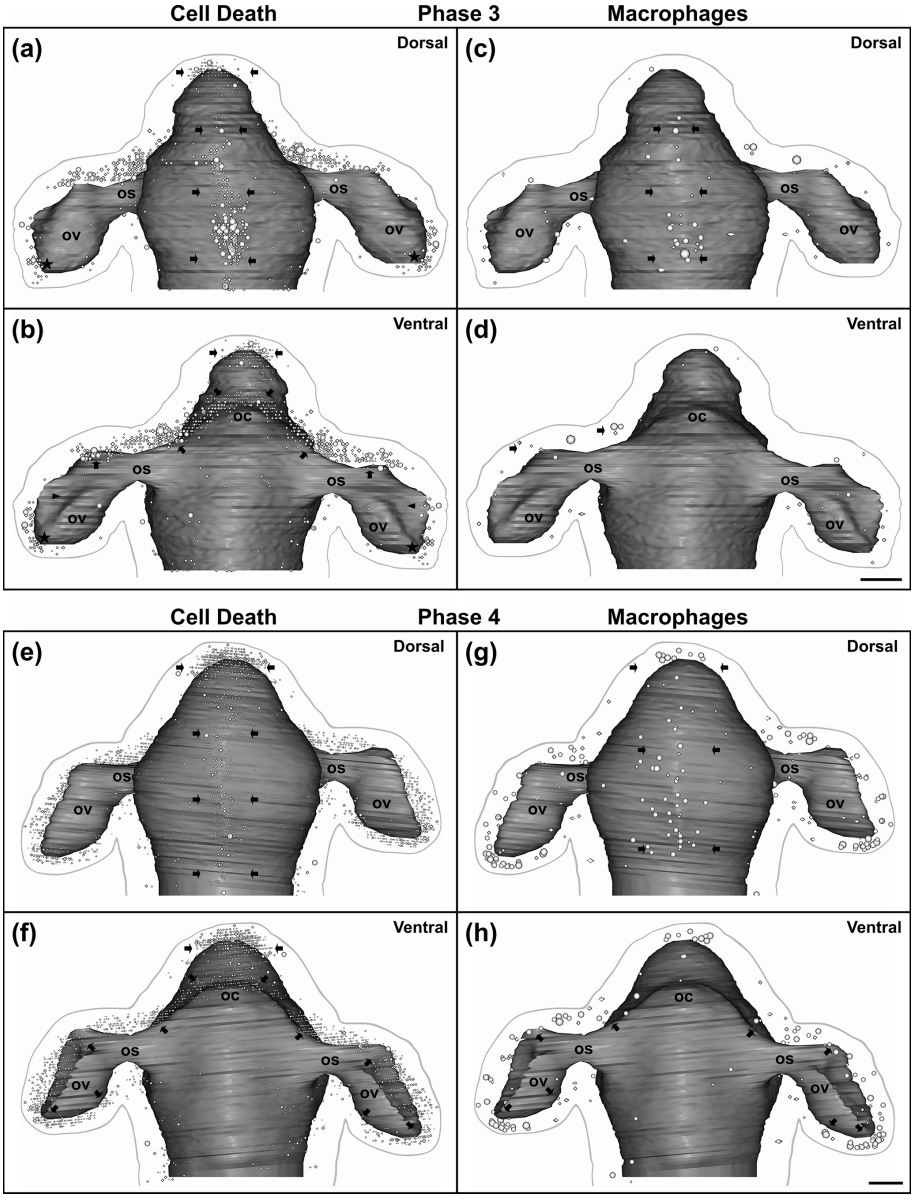

Figure 12. Apoptosis and macrophages in the developing forebrain of *Tupaia belangeri*. 3-D reconstructions demonstrate the brain ventricle (gray), the pial surface of the brain (light gray contour), and apoptotic bodies (left side: **a**, **b**, **e**, **f**) or macrophages (right side: **c**, **d**, **g**, **h**) coded as white spheres in each case. **(a–d)** Embryonic day (E) 15, phase 3 ("onset of invagination of the optic vesicle"). A band of apoptotic cells (arrows) resides in the dorsal midline of the forebrain **(a)** and proceeds (arrows) to the ventral midline of the forebrain **(b)**. In the prospective position of the optic chiasm (oc), this band splits to both optic stalks (os) and further extends to the ventrolateral walls of the optic vesicles (ov). Arrowheads, impressions of the optic ventricles due to the initial thickening of the developing retina. **(c, d)** Groups of macrophages (arrows) are found in the positions of large-scale apoptosis **(a, b)**. **(e–h)** E15, phase 4 ("advanced invagination of the optic vesicle"). **(e)** Numerous fragments of apoptotic cells are present in the dorsal midline of the forebrain (arrows). **(f)** Again, this apoptotic band continuously extends (arrows) to the ventral pole of the forebrain, to the future position of the optic chiasm and, bilaterally symmetrically, to the optic stalks; and, further, to the invaginating retinal thickenings. In the phase 4 embryo, this band terminates in the future pigment epithelium. **(g, h)** A band-like formation of macrophages (arrows) largely colocalizes with the maximally extended apoptotic band shown in **(e, f)**. Scale bars = 100 µm. Reproduced from Knabe et al. (2000, Figs. 3, 4).

6 Apoptosis and macrophages in the developing forebrain and eyes

The second main research area of Wolfgang Knabe and colleagues, whose roots date back to the former anatomical department of Hans-Jürg Kuhn, continued previous projects on the retina, then served as a bridge between the retina and the forebrain, and, thereafter, was successively expanded to include the entire brain, spinal cord, neural crest, and the placodes.

As conflicting statements had been published with regard to the patterns and functions of apoptosis in the early developing forebrain and eye, we decided to further study this issue using 3-D reconstructions. For this purpose "semithin" serial sections, meaning sections from 1 to 2 µm in thickness, were taken from young embryos of *Tupaia belangeri*. In contrast to the work of earlier authors which had postulated the ubiquitous existence of isolated foci of cell death, we observed a spatiotemporally continuous process with a sharply defined maximum and characteristic, long-drawn-out "bands of apoptotic cells". Most, if not all, isolated apoptotic foci – which previously had been reported and, partly, interpreted as species-specific characters by others – turned out to topographically represent "segments" of a maximally extended band of cell death resembling that found in *Tupaia belangeri*. We, therefore, concluded that at least similar band-like apoptotic processes should occur in the embryonic forebrain and eyes of other vertebrates (Knabe and Kuhn, 1998b; Knabe et al., 2000).

In *Tupaia belangeri*, the maximally extended band of apoptotic cells runs from the dorsal to the ventral midline of the prosencephalon (Fig. 12a, c, e, g). From the approximate future position of the optic chiasm, this band continues, bilaterally symmetrically, to the lateral wall of the diencephalon, to the optic stalk, and, finally, to the ventral, lateral, and dorsal walls of the invaginating optic vesicle (Knabe et al., 2000). Supported by additional other evidence (Golden et al., 1999), the long-drawn-out band of developmental cell death discovered by us appears to contribute to the regulation of late bilateralization processes of the forebrain which, finally, help to establish paired hemispheres of the forebrain as well as paired olfactory and optic anlagen. Consequently, disturbances of the physiological pattern of apoptosis may cause holoprosencephaly and cyclopia, or related malformations.

Given the fact that professional macrophages can eliminate dead cells or trigger apoptosis (Frade and Barde, 1998; Diez-Roux et al., 1999; for a review, see Pont-Lezica et al., 2011), we were interested to learn whether macrophages influence apoptosis in the early developing forebrain and eyes of *Tupaia belangeri*. It came out that, in Tupaia, earliest macrophages are present in the blood islands of the yolk sac. Thereafter, macrophages emigrate from the perineural vessels, invade the anlagen of the forebrain and eyes from their pial/external surfaces, transmigrate the neuroepithelial wall, and, finally, arrive in the developing brain ventricles (Fig. 13a–d, Knabe and Kuhn, 1999).

An early appearance of macrophages was also demonstrated in the brain and optic anlagen of zebrafish (Phelan et al., 2005). These macrophages express members of the evolutionarily conserved Toll-like family (zfTLR3, zflRAK-4, and zfTRAF6) which is of relevance for the innate immune system. Resembling our findings in *Tupaia belangeri*, primitive macrophages invade the zebrafish brain prior to its vascularization (for a review, see Traver et al., 2003). However, whether macrophage colonization of the brain follows the same principle in mammals and birds remains a matter of debate. Thus, in chicks, Kurz et al. (2001) found evidence that "blood-borne cells do not contribute to the intraneural macrophage population of the embryonic CNS" – at least during the time window which can be studied in chick–quail parabiosis.

Standardized counts in the embryos of *Tupaia belangeri* revealed that "waves of macrophages", which all in all reflect their invasion route, occur sequentially in the different perineural compartments and, with a delay, in the neuroepithelium (Fig. 13e). Our 3-D reconstructions further demonstrate that macrophages rapidly invade pre-existing bands of apoptotic cells (Fig. 12). There is no indication for the induction of large-scale apoptosis by macrophages (Knabe and Kuhn, 1999; Knabe et al., 2000). A close association between cell death and macrophages was also found in early phases, but not in late phases, of mouse retinal development (Santos et al., 2008).

The question whether, in vertebrates, a "canon" of apoptotic patterns exists in certain phases of brain development has lost none of its immediacy. This applies all the more so since, in particular, the functions of apoptotic events in early developmental periods are still poorly understood. Bejarano-Escobar et al. (2013), for example, are studying the small spotted catshark *Scyliorhinus canicula*, first because elasmobranchs "occupy a key phylogenetic position as an outgroup to osteichthyans" and, second, because catsharks grow slowly and have large eyes, the latter properties being of great benefit for the analysis of rapidly running apoptotic processes. It turned out that apoptotic events in dorsal parts of the optic vesicle – initially judged to be a specific property of the chick (García-Porrero et al., 1984) and, later, demonstrated in *Tupaia belangeri* (Knabe and Kuhn, 1998b; Knabe et al. 2000) – are also present in the catshark (Bejarano-Escobar et al., 2013). Correspondence between *Tupaia belangeri* and *Scyliorhinus canicula* also exists regarding clusters of apoptotic cells in the anterior wall of the developing lens as well as in the future position of the optic chiasm where apoptosis probably contributes to the ventral shifting of the optic stalk. However, no match was found for the "suboptic necrotic center" (SONC, Källén, 1965; Navascués et al., 1988), which, in the vicinity of the optic chiasm, is particularly conspicuous in *Tupaia belangeri*. Fully in line with this, no chronotopographical relationship be-

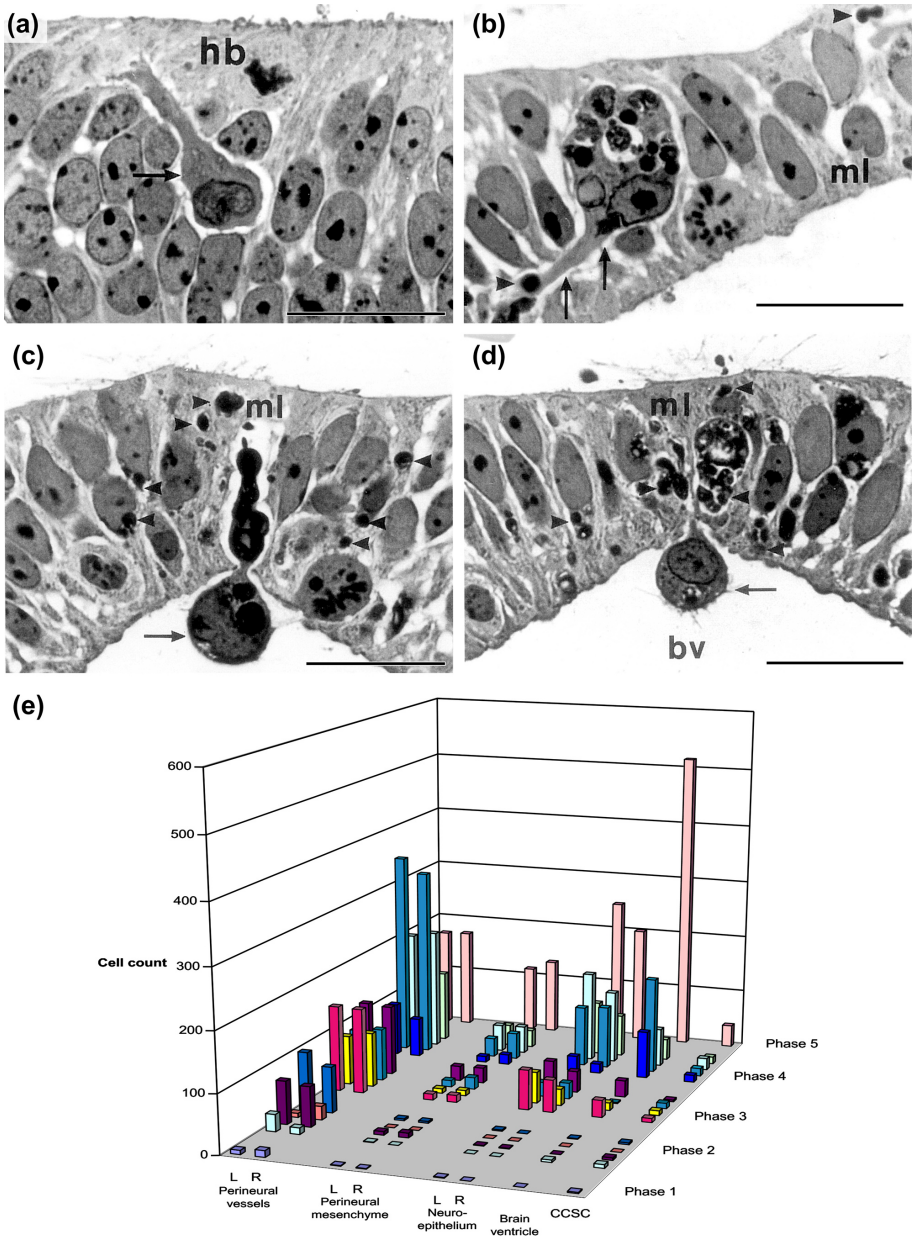

Figure 13. Earliest occurrence of macrophages in the developing brain of *Tupaia belangeri*. **(a–d)** Semithin sections stained with hematoxylin (Heidenhain) from phase 3 (**a**, "onset of invagination of the optic vesicle") and phase 4 (**b–d**, "advanced invagination of the optic vesicle"). **(a)** Lateral wall of the hindbrain (hb): migrating macrophages (arrow) are surrounded by a distinct halo. **(b)** Midline (ml) of the forebrain: an intramural macrophage is filled with phagosomes and extends pseudopods (arrows) to phagocytize apoptotic bodies (arrowheads). **(c, d)** Intraventricular macrophages (arrows) in contact with the neuroepithelium. Arrowheads, apoptotic bodies; bv, brain ventricle. **(e)** Macrophages in perineural and neural compartments of Tupaia embryos which were classified according to five phases of ocular development. Except for the brain ventricle and the central canal of the spinal cord (CCSC), macrophages were separately counted for left and right sides of the brain. Scale bars = 20 µm. Reproduced from Knabe and Kuhn (1999, Figs. 2a, 3e–f, 4a, b).

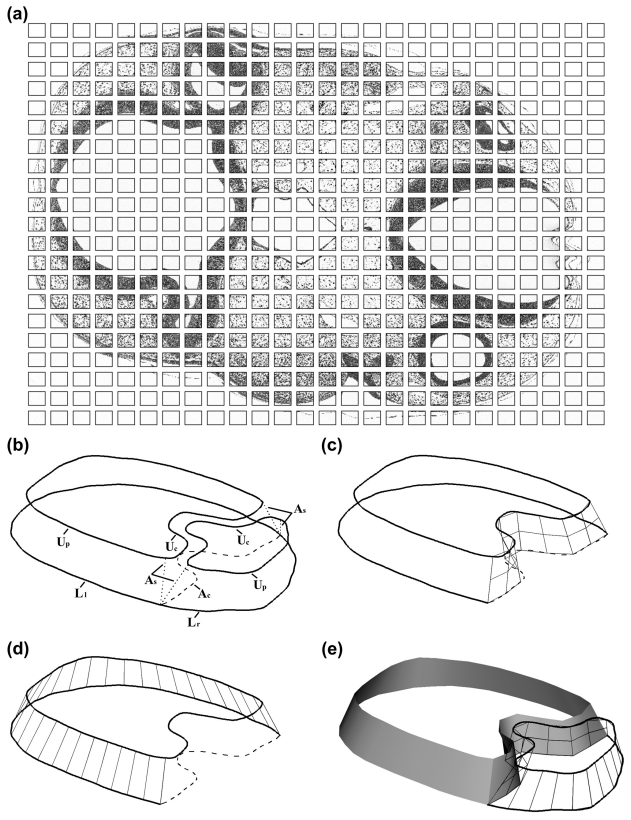

Figure 14. High-resolution scanning and computer-aided 3-D reconstructions of cellular events in the nervous system of *Tupaia belangeri*. **(a)** Composition of a single high-resolution image acquired with the scanning system "Huge Image" from a semithin section (section thickness: 1 µm) of a 15-day-old Tupaia embryo. Each of the 546 single small images is scanned with the ×100 objective lens to facilitate structural diagnosis of apoptotic cells. **(b–e)** In the vector-based software AutoCAD, 3-D reconstructions are created by generating surfaces between corresponding polylines which represent the contours of organ anlagen. **(b)** To generate surfaces for a y-shaped object, both polylines are split into peripheral (U_p) and central (U_c) parts in the upper plane. In the lower plane, a curved auxiliary line (A_c) divides the polyline into left (L_l) and right (L_r) parts. **(c)** Straight auxiliary lines (A_s) help to create edge surfaces in central parts of the contours. **(d)** Next, rule surfaces are generated between peripheral parts of the contours. **(e)** Following surface generation, surfaces are rendered (left side of the scheme). Reprinted from Süss et al. (2002, Figs. 1a, 5). © 2002, with permission from Elsevier.

tween macrophages and apoptotic cells could be demonstrated in the catshark (Bejarano-Escobar et al., 2013). For these and other reasons, Francisco-Morcillo et al. (2014) conclude that, in the developing visual system, "dying cells show similar but not identical spatiotemporally restricted patterns in different vertebrates". The same appears to hold true for macrophages, which may or may not contribute to the elimination of apoptotic cells.

7 3-D reconstruction techniques

For a long time, 3-D reconstruction techniques have enriched the treasury of embryological research. It therefore comes as no surprise that many of the works carried out by former students of Hans-Jürg Kuhn still involve 3-D reconstructions (e.g., Schunke and Zeller, 2010; Washausen and Knabe, 2013). However, the need for processing ever bigger data sets, which in our case contain information from large embryonic surfaces as well as from millions of single cells, required a fundamental revision of our pre-existing reconstruction techniques (Knabe and Kuhn, 1996a). Similarly, elaborate atlases on prenatal organ development have been generated by other work groups (e.g., Radlanski et al., 2010).

For our purposes, we have established an AutoCAD-based reconstruction system (Knabe et al., 2000; Süss et al., 2002: Fig. 14a–d), which subsequently was optimized with the help of the Deutsche Forschungsgemeinschaft (KN 525/1-1, 1-2, BR 1185/4-1). As a first step, the novel high-resolution scanning system "Huge Image" was developed in cooperation with ZEISS (Süss et al., 2000, 2002; Fig. 14e). In line with this trend, Ma et al. (2008a, b) have established "Autostitch" to automatically combine multiple images of microscopic sections "to produce a panorama of larger image" without any time-consuming user input. Meanwhile, abundant applications of mosaic-like scanning techniques are found in biological research, e.g., in cortical mapping (Schleicher et al., 2009).

In a second step, we then developed a novel procedure for the alignment of (resin-embedded) serial sections which is largely independent of internal embryonic fiducial markers (Fig. 15). This method is especially suitable for reconstructing small embryos in utero as well as genetically modified and potentially malformed embryos which may lack relevant internal fiducial markers, e.g., symmetrically aligned organ rudiments and/or midline structures (Fig. 16, Knabe et al., 2002).

When resin-embedded tissue blocks are not available, sections from paraffin-embedded tissue may alternatively be processed by the tissue array procedure. Here, tissue cores from a donor block are embedded as fiducial markers at the periphery or inside the target tissue (Bussolati et al., 2005). To avoid complex realignment procedures, large-volume 3-D reconstruction may be coped by mounting samples on a high-precision translation stage and acquiring optical sections from the stained block surface which is sequentially removed with an ultramiller (Gerneke et al., 2007). Alternatively, non-deparaffinized thick sections which preserve mutual relationships of tissue components may be used for 3-D reconstruction with the help of either fluorescence or confocal microscopy (Jirkovská et al., 2005).

Finally, our cooperation with Guido Brunnett (Technische Universität Chemnitz) resulted in the development of a substantially faster reconstruction technique which is based on triangulation algorithms (Brunnett et al., 2003). Further joint

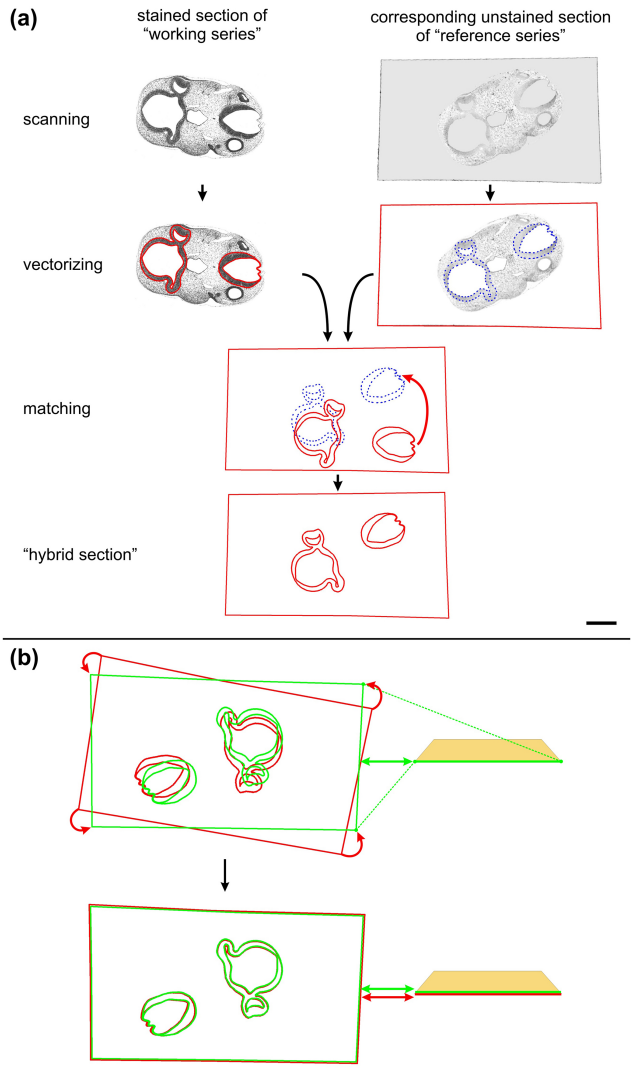

Figure 15. Realignment of histological serial sections with the help of external fiducials to build up 3-D reconstructions of apoptotic cells in the nervous system of *Tupaia belangeri*. **(a)** Semithin sections (1 µm) of a 15-day-old Tupaia embryo were alternately placed on two sets of slides. Sections from the "working series" stained with hematoxylin (Heidenhain) were scanned at high resolution (×100 objective lens, "Huge Image") and were used for vectorization of apoptotic bodies (not shown) and contours of the developing brain (red contours). Adjacent unstained sections from the "reference series" were scanned at low resolution (×5 objective lens) and were used for vectorization of the contours of the embedding block (red block contours). The vectorized embryonic contours are matched to the unstained section (dashed blue lines) and are then fused with the block contours to create a "hybrid section". **(b)** Hybrid sections are realigned with the help of the contours of the embedding block. The lower hybrid section (red) is matched to the upper one (green). Right side of the scheme: positions of the two hybrid sections in the pyramid-shaped stack of realigned hybrid sections. Scale bar = 500 µm. Reprinted from Knabe et al. (2002, Figs. 2, 3a). © 2002, with permission from Elsevier.

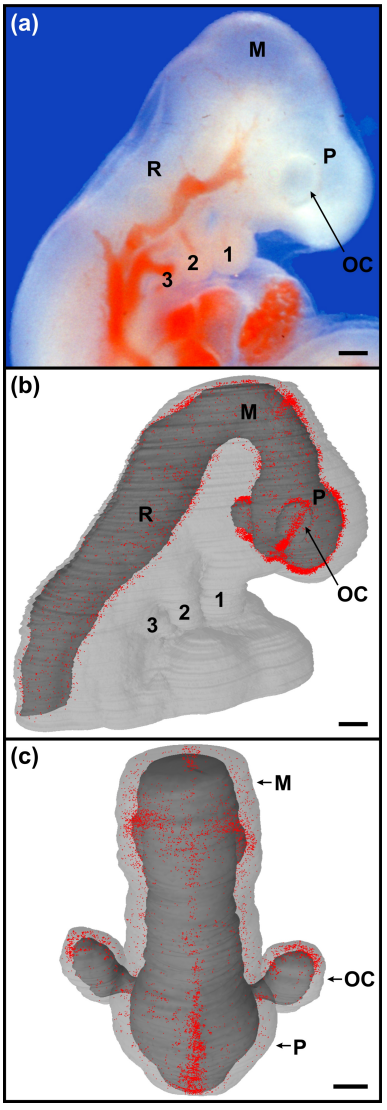

Figure 16. 3-D reconstruction of apoptotic cells in the brain of a 15-day-old embryo of *Tupaia belangeri*, serial section alignment done with "hybrid sections". **(a)** Photograph of the unsectioned translucent embryo revealing red colored blood cells in developing vessels and heart. M, mesencephalon; OC, optic cup; P, prosencephalon; R, rhombencephalon; 1, 2, 3, branchial arches 1–3. **(b, c)** 3-D reconstruction built up from semithin sections (1 µm) demonstrates the surface ectoderm (transparent light gray), the inner margin of the neuroepithelium (dark gray), and individually marked apoptotic bodies (red dots). Lateral **(b)** and frontal **(c)** views reveal a band of apoptotic cells extending from the dorsal midline of the mes- and prosencephalon to the ventral midline of the prosencephalon and, bilaterally symmetrically, to the optic cups. Note horizontal apoptotic bands at the transition from mes- to prosencephalon. Scale bars = 200 µm. Reprinted from Knabe et al. (2002, Fig. 5). © 2002, with permission from Elsevier.

projects led to improvements regarding (1) data processing, (2) calculation of the reconstruction, (3) post-processing, and (4) visualization (Kienel et al., 2008). In its current configuration, our reconstruction system calculates large embryonic surfaces, for example the outer wall of the brain and spinal cord, within just a few seconds.

8 Midbrain

By application of the optimized reconstruction system we were able to demonstrate that long-drawn-out bands of apoptotic cells are present not only in the forebrain but also in all other major divisions of the brain. For example, apoptotic events which in *Tupaia belangeri* possibly contribute to forebrain bilateralization (Knabe et al., 2000) are transiently connected to a band of dead cells in the dorsal midline of the midbrain. Additionally, there is clearly continuity with so-far-undescribed, transversely oriented bands of cell death which, bilaterally symmetrically, run at the boundary between midbrain and synencephalon (Fig. 16). Possible functions of these transverse bands may include boundary formation between developing diencephalic and mesencephalic regions and/or the elimination of precursor cells of the mesencephalic trigeminal nucleus which, in mice, is protected by the embryonic erythropoietin system (Knabe et al., 2002, 2004a).

9 Hindbrain

Previously undescribed patterns of apoptosis were also found in the rhombomeres of *Tupaia belangeri* (Knabe et al., 2004b). We wished to clarify whether segment-specific large-scale apoptosis, first noted in the chick (Lumsden et al., 1991; Jeffs et al., 1992; Graham et al., 1993, 1994; Ellies et al., 2000), is in fact generally absent from the rhombomeres of mammals (Trainor et al., 2002). Our reconstructions clearly rebut this presumption. Firstly, several identical key elements of a strictly spatiotemporally regulated sequence of apoptotic events are present in chick embryos as well as in *Tupaia belangeri* (Fig. 17). Secondly, again in line with previous findings in the chick, large-scale apoptosis in dorsal parts of rhombomere 3 and, with a delay, in rhombomere 5 occurs in parallel with the delamination of neural crest cells which, in the rostrocaudal direction, proceeds from rhombomeres 2 to 4 to 6 (Figs. 17, 18). These findings suggest that apoptosis in rhombomeres 3 and 5 predominantly eliminates premigratory neural crest cells and thereby helps to generate crest-free spaces which separate neural crest streams adjacent to the even-numbered rhombomeres. Obviously, additional factors are in place to maintain the stereotypical pattern of three spatially segregated streams of neural crest cells, for example, local cell-to-cell and long-range cell–environment interactions (Teddy and Kulesa, 2004; for a review see Theveneau and Mayor, 2012). Thirdly, except for dorsal apoptosis,

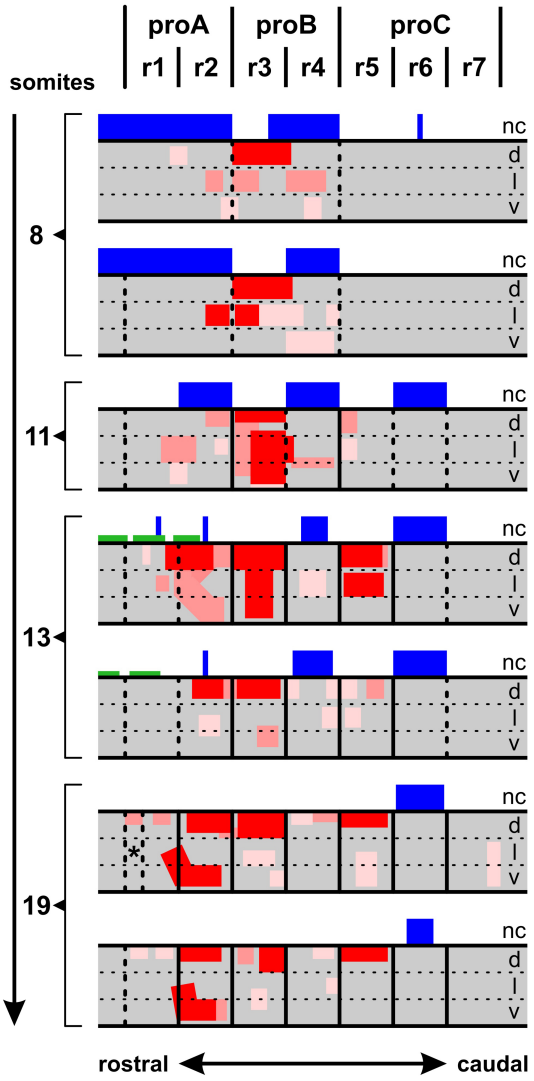

Figure 17. Segment-specific patterns of cell death and neural crest delamination in the developing hindbrain of *Tupaia belangeri*. Schemes were created from 3-D reconstructed embryos of 8 to 19 pairs of somites and show lateral views of the neuroepithelial walls (gray). Red, medium red, and light red: high, moderate, and low amounts of apoptotic cells, respectively; blue, delaminating neural crest cells (nc). Rhombomeres r1–r7 (dotted line: developing boundary; continuous line: well-demarcated boundary) develop from three pro-rhombomeres (proA, proB, proC) and are subdivided in dorsal (d), lateral (l), and ventral (v) thirds. Neural crest delamination in the even-numbered r2, r4, and r6 and apoptosis in the odd-numbered r3 and r5 (dorsal apoptotic maxima and transverse apoptotic bands) proceed rostrocaudally. Note the curved apoptotic band and the dorsal apoptotic maximum in r2. Asterisk, "rhombomere 0"; green, ventricular protrusion of fusing neural folds. Reproduced from Knabe et al. (2004b, Fig. 6).

rhombomeres 3 and 5 of the tree shrew hindbrain also contain dorsoventrally oriented apoptotic bands (Figs. 17, 18).

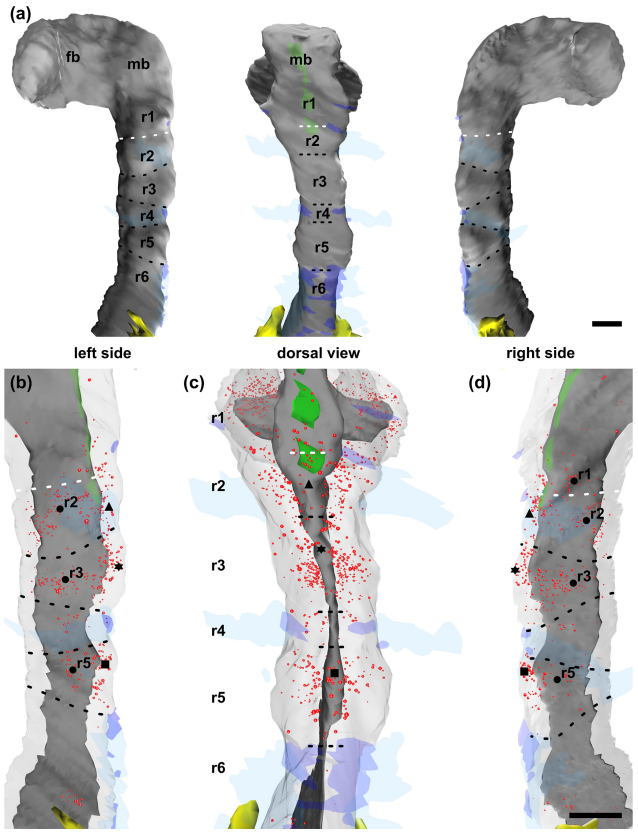

Figure 18. Segment-specific patterns of cell death and neural crest delamination in the developing hindbrain of *Tupaia belangeri*. 13-somite embryo. 3-D reconstructions demonstrate the pial (**a**: dark gray; **b–d**: light gray) or the ventricular surface (**b–d**: dark gray) of the brain (fb, forebrain; mb, midbrain; r1–r6, rhombomeres 1–6), delaminating (blue) and migrating (light blue) neural crest cells, ventricular protrusions of the fusing neural folds (green), the first somite (yellow), and individually marked apoptotic cells (red). **(a)** Definitive (black dotted lines) and less distinct (white dotted lines) interrhombomeric boundaries stand out at the pial surface of the hindbrain. **(b–d)**: left **(b)**, dorsal **(c)**, and right **(d)** views of apoptotic patterns within the hindbrain walls. Apoptotic maxima exist in dorsal parts of r3 (asterisks); r5 (rectangles); and, to a lesser extent, r2 (triangle). Note transverse apoptotic bands in r3 and r5 and curved apoptotic bands in r1/2 (black dots). Scale bars = 100 µm. Reproduced from Knabe et al. (2004b, Fig. 4). © Springer-Verlag 2004, with kind permission from Springer Science and Business Media.

They may eliminate precursors of neural crest cells which, by transplantation experiments, have been identified in these ventral positions (Sechrist et al., 1995). Alternatively, these bands of apoptotic cells may contribute to the fact that onset of neurogenesis in the odd-numbered rhombomeres occurs with a delay, compared with the even-numbered rhombomeres (Lumsden and Keynes, 1989; Eickholt et al., 2001; Knabe et al., 2004b).

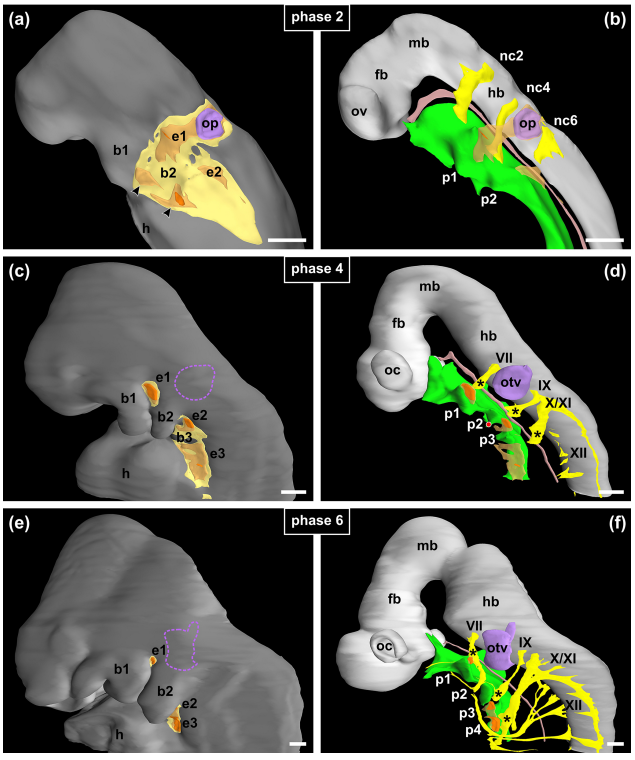

Figure 19. Morphogenesis of the epibranchial placodes and ganglia in *Tupaia belangeri*. 3-D reconstructions of 13- to 17-day-old embryos classified according to six phases of ocular development: surface ectoderm (gray) with three grades of ectodermal thickenings (1: light yellow; 2: light orange; 3: orange), brain (light gray), neural crest streams (yellow), otic anlagen (violet), endoderm (green), and notochord (light brown). **(a, c, e)** In a rostrocaudal sequence, three pairs of high-grade thickened epibranchial placodes (e1, e2, e3) develop from a common anlage with the otic placode (op). Arrowheads, presumed hypobranchial placodes; b1, b2, b3; branchial arches 1, 2, 3; h, heart. **(b, d, f)** Neural crest cells and epibranchial placodes, the latter depending on signals from the pharyngeal pouches (p1, p2, p3, p4), contribute glial or neuronal components to distinct cranial ganglia (asterisks; geniculate ganglion: VII, facial nerve; petrosal ganglion: IX, glossopharyngeal nerve; nodose ganglion: X, vagal nerve). XI, accessory nerve; XII, hypoglossal nerve; fb, forebrain; hb, hindbrain; mb, midbrain; nc2, nc4, nc6; neural crest streams adjacent to rhombomeres 2, 4, and 6; oc, optic cup; otv, otic vesicle; ov, optic vesicle; red dot, perforation of branchial membrane. Scale bars = 200 µm. Reprinted from Washausen et al. (2005, Figs. 2c, d, 4a, b, e, f). © 2004, with permission from Elsevier.

10 Neurogenic placodes

Given the fact that, in *Tupaia belangeri*, premigratory neural crest cells are subjected to apoptotic selection, we wondered whether premigratory cells in neurogenic placodes which also contribute to the formation of cranial ganglia are "checked" in a similar fashion (Fig. 19). This hypothesis could be confirmed on the example of the epibranchial pla-

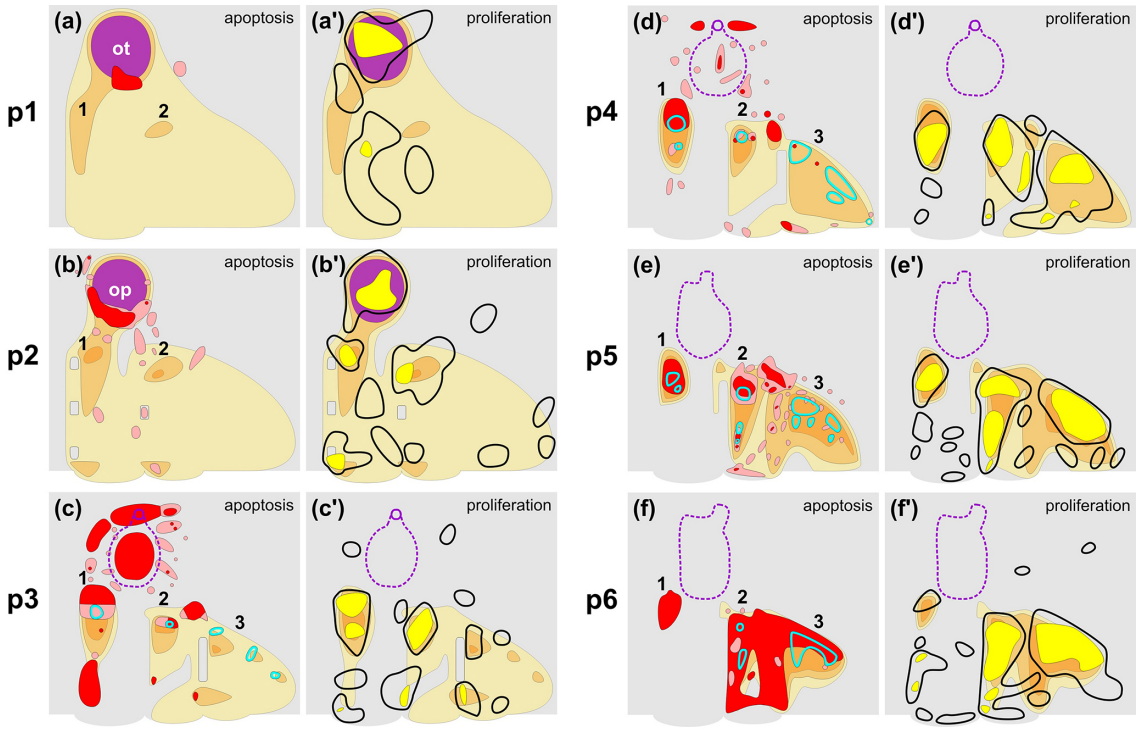

Figure 20. Apoptosis, proliferation, and neuroblast delamination in the epibranchial placodes of *Tupaia belangeri*. Schemes derived from 3-D reconstructed embryos of phases 1 to 6 (p1–p6) of ocular development: surface ectoderm (gray), three grades of ectodermal thickenings (light yellow: at least cylindrical; light orange: at least pseudostratified; orange: pseudostratified with at least three rows of nuclei), otic placode (ot) or pit (op; violet), projection of otic vesicle (dashed violet line), attachment site of otic vesicle (violet circle), apoptotic cells on one (light red) or both sides (red) of the embryonic body, hot spots of proliferation on one (thick black lines) or both sides (yellow) of the embryonic body, delaminating placodal neuroblasts (light blue). **(a–f)** Apoptotic events proceed rostrocaudally and contribute to the individualization of otic and epibranchial placodes (1, 2, 3) from their combined anlagen. In structurally demarcated epibranchial placodes, apoptosis first assists in the "selection" of premigratory placodal cells and, finally, in the regression of the placodes. **(a'–f')** Preceeding neuroblast delamination as well as apoptosis, a rostrocaudal wave of proliferation passes through the anlagen of the placodes. Reprinted from Washausen et al. (2005, Fig. 7). © 2004, with permission from Elsevier.

codes (Washausen et al., 2005). In *Tupaia belangeri*, a rostrocaudally oriented apoptotic wave passes through the combined anlagen of the otic placode and all three epibranchial placodes, and it supports three major morphogenetic steps (Fig. 20): (1) the segregation of individual placodes from larger anlagen, (2) the elimination of subpopulations of premigratory epibranchial neuroblasts along dorsoventral gradients, and (3) the ultimate elimination of the epibranchial placodes after the completion of neuroblast delamination.

Studying the morphogenesis of epibranchial placodes, we could also achieve another research objective, namely to demonstrate spatiotemporal interactions between large-scale apoptosis and proliferative events (Fig. 20). Subsequent tests will aim to clarify the regulation as well as the functions of these so-far-undescribed interactions. Interestingly, these interactions also affect the otic placode which, under the influence of fibroblast growth factor (FGF) signals, shares a common zone of origin with the epibranchial placodes (Washausen et al., 2005: *Tupaia belangeri*; Sun et al., 2007: zebrafish; Sanchez-Guardado et al., 2014: chick).

In connection with these investigations, our 3-D reconstructions unexpectedly revealed structural equivalents of hypobranchial placodes which, in *Tupaia belangeri*, are eliminated by apoptosis (Washausen et al., 2005). Previously, such neurogenic placodes which are situated ventrocaudal to the pharyngeal pouches and generate functionally unexplained ganglia had been exclusively found in amphibians (Schlosser, 2006). Neurogenic zones in ventral parts of the surface ectoderm are also interesting from another point of view. In amphioxus (cephalochordates), presumed precursors of sensory neurons, unlike the later placodal cells, do not delaminate from dorsal, but from ventral parts of the surface ectoderm. Consequently, these precursor cells – which, like hypobranchial placodes in amphibians (Schlosser, 2003), express delta – may represent the prototype of placode-derived neurons of the vertebrate cranial ganglia (Rasmussen et al., 2007).

Naturally we wished to learn whether spatiotemporally regulated waves of apoptotic and proliferative events also play significant roles during the morphogenesis of other

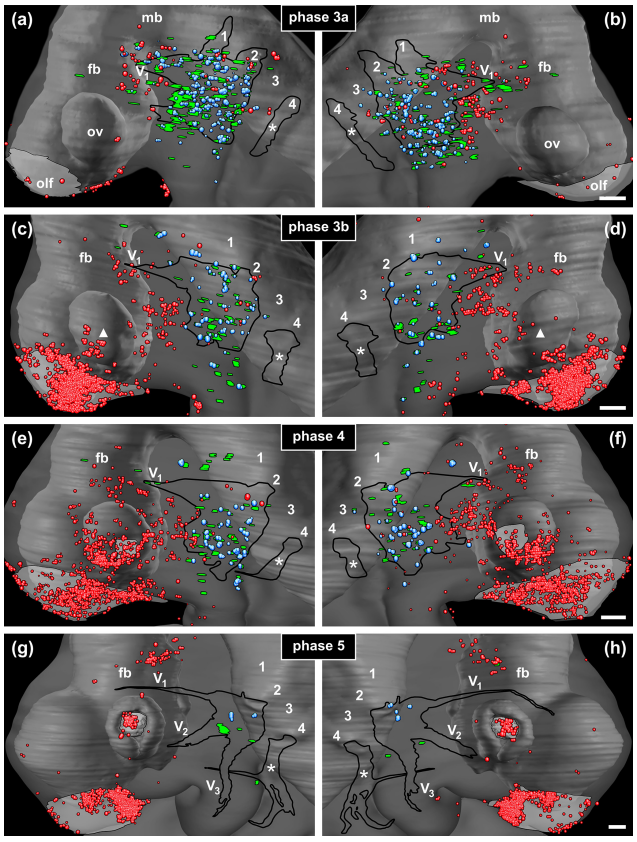

Figure 21. Apoptosis and delamination of neuroblasts in the trigeminal placode of *Tupaia belangeri*. 3-D reconstructions of embryonic heads from phases 3 to 5 of ocular development (left sides of the bodies: **a**, **c**, **e**, **g**; right sides: **b**, **d**, **f**, **h**) show apoptotic cells (red), delaminating neuroblasts (blue), and focal trigeminal placodal thickenings (green) in the surface ectoderm (transparent gray) as well as high-grade ectodermal thickenings (light gray) in the lens (triangle) and olfactory placode (olf), trigeminal ganglion and nerves (black lines, V1, V2, V3), facial nerve (black lines, asterisks), and pial brain surface (gray). **(a, b)** In the trigeminal placode, the peak of apoptosis coincides with the peak of neuroblast delamination. Simultaneously, a massive "wedge" of apoptotic cells extends ventrally from the ophthalmic trigeminal placode (position indicated by ophthalmic nerve, V1) to the presumed position of the "ventrolateral postoptic placode" postulated in chick embryos by Lee et al. (2003). **(c–f)** While low numbers of apoptotic cells persist in the regressing trigeminal placode, the apoptotic wedge merges with apoptosis being associated with the lens placode (position indicated by triangle or high-grade thickening). **(g, h)** Apoptotic cells have vanished from the former position of the trigeminal placode. 1–4, rhombomeres 1–4; fb, forebrain; mb, midbrain; ov, optic vesicle. Scale bars = 100 µm. Reproduced from Knabe et al. (2009, Fig. 6.) © the authors 2009.

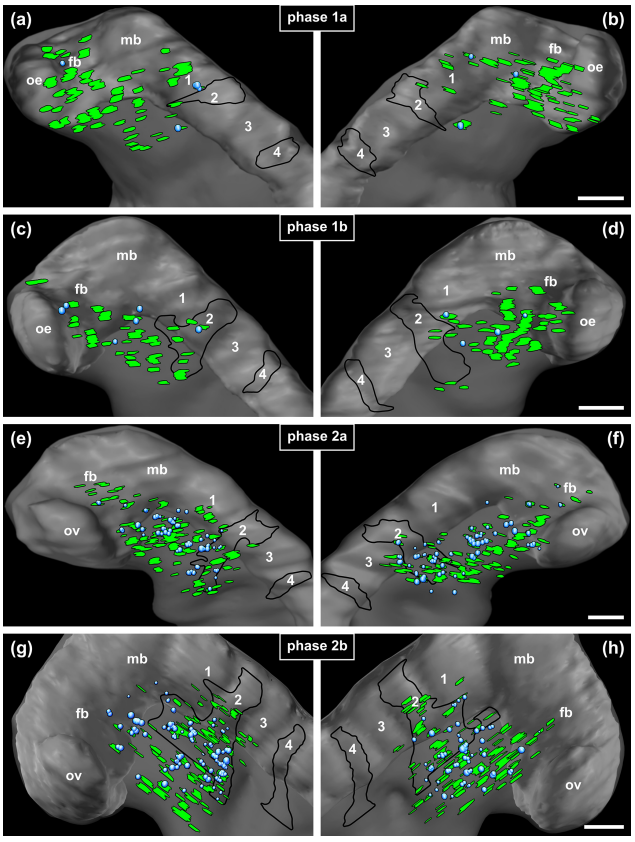

Figure 22. Early development of the trigeminal placode of *Tupaia belangeri*. 3-D reconstructions of embryonic heads from phases 1 and 2 of ocular development (left sides of the bodies: **a**, **c**, **e**, **g**; right sides: **b**, **d**, **f**, **h**) demonstrate focal trigeminal placodal thickenings (green) and delaminating placodal neuroblasts (blue) in the surface ectoderm (transparent gray), streams of neural crest cells/developing trigeminal ganglion (black lines), and pial brain surface (gray). **(a–b)** In phase 1a, the field of focal trigeminal placodal thickenings extends from positions adjacent to the forebrain (fb) to rhombomere 1 (1). **(c–h)** In phases 1b, 2a, and 2b, the placodal field is gradually shifted caudally and, now, extends from positions adjacent to the midbrain (mb) to rhombomere 3 (3). Note the increase in the number of delaminating neuroblasts. 1–4, rhombomeres 1–4; oe, optic evagination; ov, optic vesicle. Scale bars = 100 µm. Reproduced from Knabe et al. (2009, Fig. 2). © the authors 2009.

(neurogenic) placodes which segregate from the U-shaped panplacodal primordium (Streit, 2007; Schlosser, 2010; Saint-Jeannet and Moody, 2014). This hypothesis could be fully confirmed on the example of the trigeminal placode (Obermayer, 2009; Knabe et al., 2009: Fig. 21). It further emerged that even neuroblasts which migrate from the trigeminal placode to the developing trigeminal ganglion are subjected to apoptotic selection.

Our 3-D reconstructions of the trigeminal placode were also instructive with regard to the structural composition of this placode, which, in *Tupaia belangeri*, differs from all other placodes because of its diffuse texture (Fig. 22, Knabe et al., 2009). Precisely such a kind of texture as well as the striking positional changes of the vaguely delimited but contiguous trigeminal field observed in *Tupaia belangeri* also characterize the human trigeminal placode (Müller and

O'Rahilly, 2011), which, again, underlines the significance of the Tupaia model.

In the past 15 years, our knowledge on the panplacodal primordium and its derivatives has enlarged explosively. After the discovery of the basic molecular cascades which determine general and/or specific cell fates (for review, see Schlosser, 2006), brand new hypotheses on the roles of cell fate changes, local sorting-out processes, and massive cell movements await further examination (Breau and Schneider-Maunoury, 2014). Other important issues still in need of clarification are the molecular regulation and the very exact functions of large-scale apoptosis first observed during the morphogenesis of placodes in *Tupaia belangeri*. Fortunately, almost identical apoptotic patterns contribute to the development of epibranchial placodes in mice (Washausen and Knabe, 2013), which facilitates future experimental approaches.

Edited by: E. Fuchs
Reviewed by: two anonymous referees

References

Abbott, C. J., McBrien, N. A., Grünert, U., and Pianta, M. J.: Relationship of the optical coherence tomography signal to underlying retinal histology in the tree shrew (*Tupaia belangeri*), Invest. Ophthalmol. Vis. Sci., 50, 414–423, doi:10.1167/iovs.07-1197, 2009.

Abbott, C. J., Grünert, U., Pianta, M. J., and McBrien, N. A.: Retinal thinning in tree shrews with induced high myopia: Optical coherence tomography and histological assessment, Vision. Res., 51, 376–385, doi:10.1016/j.visres.2010.12.005, 2011.

Ahn, A. H., Dziennis, S., Hawkes, R., and Herrup, K.: The cloning of zebrin II reveals its identity with aldolase C, Development, 120, 2081–2090, 1994.

Ahnelt, P. K. and Kolb, H.: The mammalian photoreceptor mosaic-adaptive design, Prog. Retin. Eye Res., 19, 711–777, doi:10.1016/S1350-9462(00)00012-4, 2000.

Ahuja, P., Caffé, A. R., Ahuja, S., Ekström, P., and van Veen, T.: Decreased glutathione transferase levels in rd1/rd1 mouse retina: Replenishment protects photoreceptors in retinal explants, Neuroscience, 131, 935–943, doi:10.1016/j.neuroscience.2004.11.012, 2005.

Almsherqi, Z. A., Landh, T., Kohlwein, S. D., and Deng, Y.: Cubic membranes: The missing dimension of cell membrane organization, Int. Rev. Cell Mol. Biol., 274, 275–342, doi:10.1016/S1937-6448(08)02006-6, 2009.

Almsherqi, Z., Margadant, F., and Deng, Y.: A look through "lens" cubic mitochondria, Interface Focus, 2, 539–545, doi:10.1098/rsfs.2011.0120, 2012.

Arnason, U. and Janke, A.: Mitogenomic analyses of eutherian relationships, Cytogenet. Genome Res., 96, 20–32, doi:10.1159/000063023, 2002.

Ashwell, K. W.: Development of the olfactory pathways in platypus and echidna, Brain Behav. Evol., 79, 45–56, doi:10.1159/000332804, 2012.

Ashwell, K. W., Marotte, L. R., and Cheng, G.: Development of the olfactory system in a wallaby (*Macropus eugenii*), Brain Behav. Evol., 71, 216–230, doi:10.1159/000119711, 2008.

Bastianelli, E., Polans, A. S., Hidaka, H., and Pochet, R.: Differential distribution of six calcium-binding proteins in the rat olfactory epithelium during postnatal development and adulthood, J. Comp. Neurol., 354, 395–409, doi:10.1002/cne.903540308, 1995.

Battle, C., Ott, C. M., Burnette, D. T., Lippincott-Schwartz, J., and Schmidt, C. F.: Intracellular and extracellular forces drive primary cilia movement, Proc. Natl. Acad. Sci. USA, 112, 1410–1415, doi:10.1073/pnas.1421845112, 2015.

Bejarano-Escobar, R., Blasco, M., Durán, A. C., Martín-Partido, G., and Francisco-Morcillo, J.: Chronotopographical distribution patterns of cell death and of lectin-positive macrophages/microglial cells during the visual system ontogeny of the small-spotted catshark *Scyliorhinus canicula*, J. Anat., 223, 171–184, doi:10.1111/joa.12071, 2013.

Berger, E. R.: On the mitochondrial origin of oil drops in the retinal double cone inner segments, J. Ultrastruct. Res., 14, 143–157, doi:10.1016/S0022-5320(66)80041-2, 1966.

Bischoff, A.: Die Ontogenese der primären Schädelseitenwand von *Tupaia belangeri*, Doctoral thesis, Department of Morphology, University of Göttingen, Germany, 1989.

Blanck, H.-G.: Die Entwicklung der Hypophyse von *Tupaia belangeri* (Tupaiidae, Scandentia, Mammalia), Doctoral thesis, Department of Morphology, University of Göttingen, Germany, 1983.

Borwein, B.: The retinal receptor: A description, in: Vertebrate photoreceptor optics, edited by: Enoch, J. M., Stiles, W. S., and Tobey Jr., F. L., Springer series in optical sciences, 23, Springer, Berlin, Germany, 11–81, 1981.

Bosco, A., Cusato, K., Nicchia, G. P., Frigeri, A., and Spray, D. C.: A developmental switch in the expression of aquaporin-4 and Kir4.1 from horizontal to Müller cells in mouse retina, Invest. Ophthalmol. Vis. Sci., 46, 3869–3875, doi:10.1167/iovs.05-0385, 2005.

Breau, M. A. and Schneider-Maunoury, S.: Mechanisms of cranial placode assembly, Int. J. Dev. Biol., 58, 9–19, doi:10.1387/ijdb.130351mb, 2014.

Brochu, G., Maler, L., and Hawkes, R.: Zebrin II: A polypeptide antigen expressed selectively by Purkinje cells reveals compartments in rat and fish cerebellum, J. Comp. Neurol., 291, 538–552, doi:10.1002/cne.902910405, 1990.

Brookover, C.: The nervus terminalis in adult man, J. Comp. Neurol., 24, 131–135, doi:10.1002/cne.900240203, 1914.

Brunnett, G., Vančo, M., Haller, C., Washausen, S., Kuhn, H.-J., and Knabe, W.: Visualization of cross sectional data for morphogenetic studies, in: Informatik 2003: Innovative Informatikanwendungen, Band 1, edited by: Dittrich, K. R., König, W., Oberweis, A., Rannenberg, K., and Wahlster, W., GI-Edition: Lecture notes in informatics, P-34, Köln, Bonn, Germany, 354–359, 2003.

Bussolati, G., Marchiò, C., and Volante, M.: Tissue arrays as fiducial markers for section alignment in 3-D reconstruction technology, J. Cell. Mol. Med., 9, 438–445, doi:10.1111/j.1582-4934.2005.tb00368.x, 2005.

Castro, A., Becerra, M., Anadón, R., and Manso, M. J.: Distribution and development of FMRFamide-like immunoreactive neuronal

systems in the brain of the brown trout, *Salmo trutta fario*, J. Comp. Neurol., 440, 43–64, doi:10.1002/cne.1369, 2001.

Castro, A., Becerra, M., Manso, M. J., and Anadón, R.: Calretinin immunoreactivity in the brain of the zebrafish, *Danio rerio*: distribution and comparison with some neuropeptides and neurotransmitter-synthesizing enzymes. I. Olfactory organ and forebrain, J. Comp. Neurol., 494, 435–459, doi:10.1002/cne.20782, 2006.

Castro, A., Becerra, M., Anadón, R., and Manso, M. J.: Distribution of calretinin during development of the olfactory system in the brown trout, *Salmo trutta fario*: Comparison with other immunohistochemical markers, J. Chem. Neuroanat., 35, 306–316, doi:10.1016/j.jchemneu.2008.03.005, 2008.

Chung, S. H., Marzban, H., Croci, L., Consalez, G. G., and Hawkes, R.: Purkinje cell subtype specification in the cerebellar cortex: Early B-cell factor 2 acts to repress the zebrin II-positive Purkinje cell phenotype, Neuroscience, 153, 721–732, doi:10.1016/j.neuroscience.2008.01.090, 2008.

Collin, S. P., and Potter, I. C.: The ocular morphology of the southern hemisphere lamprey *Mordacia mordax* Richardson with special reference to a single class of photoreceptor and a retinal tapetum, Brain Behav. Evol., 55, 120–138, doi:10.1159/000006647, 2000.

Collin, S. P., Hart, N. S., Shand, J., and Potter, I. C.: Morphology and spectral absorption characteristics of retinal photoreceptors in the southern hemisphere lamprey (*Geotria australis*), Vis. Neurosci., 20, 119–130, doi:10.1017/S0952523803202030, 2003.

Croci, L., Chung, S. H., Masserdotti, G., Gianola, S., Bizzoca, A., Gennarini, G., Corradi, A., Rossi, F., Hawkes, R., and Consalez, G. G.: A key role for the HLH transcription factor EBF2$^{COE2,O/E-3}$ in Purkinje neuron migration and cerebellar cortical topography, Development, 133, 2719–2729, doi:10.1242/dev.02437, 2006.

Dawid, B.: Die Ontogenese der Chorda dorsalis von *Tupaia belangeri* (Tupaiidae, Scandentia, Mammalia), Doctoral thesis, Department of Morphology, University of Göttingen, Germany, 1989.

Dawid, E.: Die Ontogenese der Visceralbogenarterien von *Tupaia belangeri* (Tupaiidae, Scandentia, Mammalia), Doctoral thesis, Department of Morphology, University of Göttingen, Germany, 1989.

de Vries, E.: Note on the ganglion vomeronasale, K. Akad. van Wetenschappen te Amsterdam, 7, 704 pp., 1905.

Demilly, A., Reeber, S. L., Gebre, S. A., and Sillitoe, R. V.: Neurofilament heavy chain expression reveals a unique parasagittal stripe topography in the mouse cerebellum, Cerebellum, 10, 409–421, doi:10.1007/s12311-010-0156-y, 2011.

Dieterich, C. E.: Elektronenmikroskopische Untersuchungen über die Photoreceptoren und Receptorensynapsen bei reinen Stäbchen- und Zapfennetzhäuten, A. Graef. Arch. Klin. Ex., 174, 289–320, doi:10.1007/BF00406626, 1968.

Dieterich, C. E.: Die Feinstruktur der Photorezeptoren des Spitzhörnchens *Tupaia glis*, Verh. Anat. Ges., 63, 305–312, 1969.

Diez-Roux, G., Argilla, M., Makarenkova, H., Ko, K., and Lang, R. A.: Macrophages kill capillary cells in G1 phase of the cell cycle during programmed vascular regression, Development, 126, 2141–2147, 1999.

Dkhissi-Benyahya, O., Szél, A., Degrip, W. J., and Cooper, H. M.: Short and mid-wavelength cone distribution in a nocturnal Strepsirrhine primate (*Microcebus murinus*), J. Comp. Neurol., 438, 490–504, doi:10.1002/cne.1330, 2001.

Eckmiller, M. S.: Cone outer segment morphogenesis: Taper change and distal invaginations, J. Cell Biol., 105, 2267–2277, doi:10.1083/jcb.105.5.2267, 1987.

Eckmiller, M. S.: Distal invaginations and the renewal of cone outer segments in anuran and monkey retinas, Cell Tissue Res., 260, 19–28, doi:10.1007/BF00297486, 1990.

Eickhoff, S.: Die Ontogenese des Schultergürtels von *Tupaia belangeri* (Tupaiidae, Scandentia, Mammalia), Doctoral thesis, Department of Morphology, University of Göttingen, Germany, 1989.

Eickholt, B. J., Graham, A., Lumsden, A., and Wizenmann, A.: Rhombomere interactions control the segmental differentiation of hindbrain neurons, Mol. Cell. Neurosci., 18, 141–148, doi:10.1006/mcne.2001.1014, 2001.

Ellies, D. L., Church, V., Francis-West, P., and Lumsden, A.: The WNT antagonist cSFRP2 modulates programmed cell death in the developing hindbrain, Development, 127, 5285–5295, 2000.

Engelmann, R. and Peichl, L.: Unique distribution of somatostatin-immunoreactive cells in the retina of the tree shrew (*Tupaia belangeri*), Eur. J. Neurosci., 8, 220–228, doi:10.1111/j.1460-9568.1996.tb01183.x, 1996.

Ernstberger, T.: Beitrag zur Ontogenese und funktionellen Morphologie des Fußskelets der Tupaiidae: Vergleichende Untersuchungen an Tupaia und Ptilocercus (Mammalia: Scandentia), Doctoral thesis, Department of Morphology, University of Göttingen, Germany, 1994.

Famiglietti, E. V. and Sundquist, S. J.: Development of excitatory and inhibitory neurotransmitters in transitory cholinergic neurons, starburst amacrine cells, and GABAergic amacrine cells of rabbit retina, with implications for previsual and visual development of retinal ganglion cells, Vis. Neurosci., 27, 19–42, doi:10.1017/S0952523810000052, 2010.

Flamarique, I. N. and Hárosi, F. I.: Photoreceptors, visual pigments, and ellipsosomes in the killifish, *Fundulus heteroclitus*: A microspectrophotometric and histological study, Vis. Neurosci., 17, 403–420, 2000.

Foelix, R. F., Kretz, R., and Rager, G.: Structure and postnatal development of photoreceptors and their synapses in the retina of the tree shrew (*Tupaia belangeri*), Cell Tissue Res., 247, 287–297, doi:10.1007/BF00218310, 1987.

Frade, J. M. and Barde, Y. A.: Microglia-derived nerve growth factor causes cell death in the developing retina, Neuron, 20, 35–41, doi:10.1016/S0896-6273(00)80432-8, 1998.

Francisco-Morcillo, J., Bejarano-Escobar, R., Rodríguez-León, J., Navascués, J., and Martín-Partido, G.: Ontogenetic cell death and phagocytosis in the visual system of vertebrates, Dev. Dyn., 243, 1203–1225, doi:10.1002/dvdy.24174, 2014.

Fujita, H., Oh-Nishi, A., Obayashi, S., and Sugihara, I.: Organization of the marmoset cerebellum in three-dimensional space: Lobulation, aldolase C compartmentalization and axonal projection, J. Comp. Neurol., 518, 1764–1791, doi:10.1002/cne.22301, 2010.

Fujita, H., Aoki, H., Ajioka, I., Yamazaki, M., Abe, M., Oh-Nishi, A., Sakimura, K., and Sugihara, I.: Detailed expression pattern of aldolase C (Aldoc) in the cerebellum, retina and other areas

of the CNS studied in Aldoc-Venus knock-in mice, PLoS One, 9, e86679, doi:10.1371/journal.pone.0086679, 2014.

Funke, C.: Die Entwicklung der Arterien der unteren Extremität bei *Tupaia belangeri* (Tupaiidae, Scandentia, Mammalia), Doctoral thesis, Department of Morphology, University of Göttingen, Germany, 1995.

Funke, C. and Kuhn, H.-J.: The morphogenesis of the arteries of the pelvic extremity: A comparative study of mammals with special reference to the tree shrew *Tupaia belangeri* (Tupaiidae, Scandentia, Mammalia), edited by: Beck, F., Brown, D., Christ, B., Kriz, W., Marani, E., Putz, R., Sano, Y., Schiebler, T. H., and Zilles, K., Springer, Berlin, Germany, Adv. Anat. Embryol. Cell Biol., 144, 97 pp., 1998.

Gakovic, M., Shu, X., Kasioulis, I., Carpanini, S., Moraga, I., and Wright, A. F.: The role of RPGR in cilia formation and actin stability, Hum. Mol. Genet., 20, 4840–4850, doi:10.1093/hmg/ddr423, 2011.

García-Porrero, J. A., Colvée, E., and Ojeda, J. L.: Cell death in the dorsal part of the chick optic cup. Evidence for a new necrotic area, J. Embryol. Exp. Morphol., 80, 241–249, 1984.

Garrett, E. C., Dennis, J. C., Bhatnagar, K. P., Durham, E. L., Burrows, A. M., Bonar, C. J., Steckler, N. K., Morrison, E. E., and Smith, T. D.: The vomeronasal complex of nocturnal strepsirhines and implications for the ancestral condition in primates, Anat. Rec. (Hoboken), 296, 1881–1894, doi:10.1002/ar.22828, 2013.

Gastinger, M. J., Singh, R. S., and Barber, A. J.: Loss of cholinergic and dopaminergic amacrine cells in streptozotocin-diabetic rat and $Ins2^{Akita}$-diabetic mouse retinas, Invest. Ophthalmol. Vis. Sci., 47, 3143–3150, doi:10.1167/iovs.05-1376, 2006.

Germer, A., Schuck, J., Wolburg, H., Kuhrt, H., Mack, A. F., and Reichenbach, A.: Distribution of mitochondria within Müller cells – II. Post-natal development of the rabbit retinal periphery *in vivo* and *in vitro*: Dependence on oxygen supply, J. Neurocytol., 27, 347–359, doi:10.1023/A:1006938825474, 1998.

Gerneke, D. A., Sands, G. B., Ganesalingam, R., Joshi, P., Caldwell, B. J., Smaill, B. H., and Legrice, I. J.: Surface imaging microscopy using an ultramiller for large volume 3-D reconstruction of wax- and resin-embedded tissues, Microsc. Res. Tech., 70, 886–894, doi:10.1002/jemt.20491, 2007.

Golden, J. A., Bracilovic, A., McFadden, K. A., Beesley, J. S., Rubenstein, J. L., and Grinspan, J. B.: Ectopic bone morphogenetic proteins 5 and 4 in the chicken forebrain lead to cyclopia and holoprosencephaly, Proc. Natl. Acad. Sci. USA, 96, 2439–2444, doi:10.1073/pnas.96.5.2439, 1999.

Graham, A., Heyman, I., and Lumsden, A.: Even-numbered rhombomeres control the apoptotic elimination of neural crest cells from odd-numbered rhombomeres in the chick hindbrain, Development, 119, 233–245, 1993.

Graham, A., Francis-West, P., Brickell, P., and Lumsden, A.: The signalling molecule BMP4 mediates apoptosis in the rhombencephalic neural crest, Nature, 372, 684–686, doi:10.1038/372684a0, 1994.

Hailman, J. P.: Oildroplets in the eyes of adult anuran amphibians: A comparative survey, J. Morphol., 148, 453–468, doi:10.1002/jmor.1051480404, 1976.

Halpern, M. and Martínez-Marcos, A.: Structure and function of the vomeronasal system: an update, Prog. Neurobiol., 70, 245–318, doi:10.1016/S0301-0082(03)00103-5, 2003.

Hardisty, M. W.: Lampreys and hagfishes: Analysis of cyclostome relationships, in: The biology of lampreys, edited by: Hardisty, M. W. and Potter, I. C., Academic Press, London, UK, 85–125, 1982.

Harman, A. M. and Jeffery, G.: Development of the chiasm of a marsupial, the quokka wallaby, J. Comp. Neurol., 359, 507–521, doi:10.1002/cne.903590311, 1995.

Hárosi, F. I. and Novales Flamarique, I.: Functional significance of the taper of vertebrate cone photoreceptors, J. Gen. Physiol., 139, 159–187, doi:10.1085/jgp.201110692, 2012.

Hawkes, R. and Leclerc, N.: Purkinje cell axon collateral distributions reflect the chemical compartmentation of the rat cerebellar cortex, Brain Res., 476, 279–290, doi:10.1016/0006-8993(89)91248-1, 1989.

Heizmann, C. W. and Braun, K.: Changes in Ca^{2+}-binding proteins in human neurodegenerative disorders, Trends Neurosci., 15, 259–264, doi:10.1016/0166-2236(92)90067-I, 1992.

Herrmann, U.: Frühentwicklung (Befruchtung und Furchung) bei *Tupaia belangeri*, Doctoral thesis, Department of Morphology, University of Göttingen, Germany, 1982.

Hoang, Q. V., Linsenmeier, R. A., Chung, C. K., and Curcio, C. A.: Photoreceptor inner segments in monkey and human retina: mitochondrial density, optics, and regional variation, Vis. Neurosci., 19, 395–407, doi:10.1017/S0952523802194028, 2002.

Holcman, D. and Korenbrot, J. I.: Longitudinal diffusion in retinal rod and cone outer segment cytoplasm: the consequence of cell structure, Biophys. J., 86, 2566–2582, doi:10.1016/S0006-3495(04)74312-X, 2004.

Hopkins, J., Fowler, R., Krishna, S., Wilson, I., Mitchell, G., and Bannister, L.: The plastid in *Plasmodium falciparum* asexual blood stages: A three-dimensional ultrastructural analysis, Protist, 150, 283–295, doi:10.1016/S1434-4610(99)70030-1, 1999.

Immel, J. H. and Fisher, S. K.: Cone photoreceptor shedding in the tree shrew (*Tupaia belangeri*), Cell Tissue Res., 239, 667–675, doi:10.1007/BF00219247, 1985.

Insinna, C. and Besharse, J. C.: Intraflagellar transport and the sensory outer segment of vertebrate photoreceptors, Dev. Dyn., 237, 1982–1992, doi:10.1002/dvdy.21554, 2008.

Ishikawa, T. and Yamada, E.: Atypical mitochondria in the ellipsoid of the photoreceptor cells of vertebrate retinas, Invest. Ophthalmol., 8, 302–316, 1969.

Iwaniuk, A. N., Marzban, H., Pakan, J. M., Watanabe, M., Hawkes, R., and Wylie, D. R.: Compartmentation of the cerebellar cortex of hummingbirds (Aves: Trochilidae) revealed by the expression of zebrin II and phospholipase Cβ4, J. Chem. Neuroanat., 37, 55–63, doi:10.1016/j.jchemneu.2008.10.001, 2009.

Janečka, J., Miller, W., Pringle, T., Wiens, F., Zitzmann, A., Helgen, K., Springer, M., and Murphy, W.: Molecular and genomic data identify the closest living relative of primates, Science, 318, 792–794, doi:10.1126/science.1147555, 2007.

Jeffery, G. and Erskine, L.: Variations in the architecture and development of the vertebrate optic chiasm, Prog. Retin. Eye Res., 24, 721–753, doi:10.1016/j.preteyeres.2005.04.005, 2005.

Jeffery, G., Harman, A., and Flügge, G.: First evidence of diversity in eutherian chiasmatic architecture: Tree shrews, like marsupials, have spatially segregated crossed and uncrossed chiasmatic pathways, J. Comp. Neurol., 390, 183–193, doi:10.1002/(SICI)1096-9861(19980112)390:2<183::AID-CNE2>3.0.CO;2-Y, 1998.

Jeffery, G., Levitt, J. B., and Cooper, H. M.: Segregated hemispheric pathways through the optic chiasm distinguish primates from rodents, Neuroscience, 157, 637–643, doi:10.1016/j.neuroscience.2008.09.021, 2008.

Jeffs, P., Jaques, K., and Osmond, M.: Cell death in cranial neural crest development, Anat. Embryol., 185, 583–588, doi:10.1007/BF00185617, 1992.

Jerxsen, R.: Ontogenese des Gebisses von *Tupaia belangeri*, Doctoral thesis, Department of Morphology, University of Göttingen, Germany, 1982.

Jia, C. and Halpern, M.: Calbindin D28K immunoreactive neurons in vomeronasal organ and their projections to the accessory olfactory bulb in the rat, Brain Res., 977, 261–269, doi:10.1016/S0006-8993(03)02693-3, 2003.

Jia, C. and Halpern, M.: Calbindin D28k, parvalbumin, and calretinin immunoreactivity in the main and accessory olfactory bulbs of the gray short-tailed opossum, *Monodelphis domestica*, J. Morphol., 259, 271–280, doi:10.1002/jmor.10166, 2004.

Jirkovská, M., Náprstková, I., Janácek, J., Kucera, T., Macásek, J., Karen, P., and Kubínová, L.: Three-dimensional reconstructions from non-deparaffinized tissue sections, Anat. Embryol., 210, 163–173, doi:10.1007/s00429-005-0006-8, 2005.

Joffe, B., Peichl, L., Hendrickson, A., Leonhardt, H., and Solovei, I.: Diurnality and nocturnality in primates: An analysis from the rod photoreceptor nuclei perspective, Evol. Biol., 41, 1–11, doi:10.1007/s11692-013-9240-9, 2014.

Johnston, J. B.: The nervus terminalis in man and mammals, Anat. Rec., 8, 185–198, doi:10.1002/ar.1090080402, 1914.

Källén, B.: Degeneration and regeneration in the vertebrate central nervous system during embryogenesis, Prog. Brain Res., 14, 77–96, doi:10.1016/S0079-6123(08)63740-1, 1965.

Kakuta, S., Oda, S., Gotoh, Y., and Kishi, K.: Calbindin-D28k and calretinin immunoreactive neurons in the olfactory bulb of the musk shrew, *Suncus murinus*, Brain Res. Dev. Brain Res., 129, 11–25, doi:10.1016/S0169-328X(01)00111-5, 2001.

Kern, T. S. and Barber, A. J.: Retinal ganglion cells in diabetes, J. Physiol., 586, 4401–4408, doi:10.1113/jphysiol.2008.156695, 2008.

Kienel, E., Vančo, M., Brunnett, G., Kowalski, T., Clauß, R., and Knabe, W.: A framework for the visualization of cross sectional data in biomedical research, in: Visualization in medicine and life sciences, edited by: Linsen, L., Hagen, H., and Hamann, B., Mathematics and visualization Springer, Berlin, Germany, 77–97, 2008.

Kim, J., Lee, E., Chang, B. S., Oh, C. S., Mun, G. H., Chung, Y. H., and Shin, D. H.: The presence of megamitochondria in the ellipsoid of photoreceptor inner segment of the zebrafish retina, Anat. Histol. Embryol., 34, 339–342, doi:10.1111/j.1439-0264.2005.00612.x, 2005.

Kim, J. Y., Marzban, H., Chung, S. H., Watanabe, M., Eisenman, L. M., and Hawkes, R.: Purkinje cell compartmentation of the cerebellum of microchiropteran bats, J. Comp. Neurol., 517, 193–209, doi:10.1002/cne.22147, 2009.

Kim, Y. K., Kim, J. H., Yu, Y. S., and Ko, H. W.: Localization of primary cilia in mouse retina, Acta Histochem., 115, 789–794, doi:10.1016/j.acthis.2013.03.005, 2013.

Kimura, Y. and Furukawa, M.: Calretinin immunoreactivity in olfactory bulb and mucosa in mice, Nihon Jibiinkoka Gakkai Kaiho, 101, 620–626, 1998.

Kinzinger, J. H., Johnson, E. W., Bhatnagar, K. P., Bonar, C. J., Burrows, A. M., Mooney, M. P., Siegel, M. I., and Smith, T. D.: Comparative study of lectin reactivity in the vomeronasal organ of human and nonhuman primates, Anat. Rec. A Discov. Mol. Cell. Evol. Biol., 284, 550–560, doi:10.1002/ar.a.20194, 2005.

Klammler, M.: Die Ontogenese der Vena cardinalis posterior bei *Tupaia belangeri* unter besonderer Berücksichtigung der frühen Stadien, Doctoral thesis, Department of Morphology, University of Göttingen, Germany, 1990.

Kloc, M., Bilinski, S., Dougherty, M. T., Brey, E. M., and Etkin, L. D.: Formation, architecture and polarity of female germline cyst in *Xenopus*, Dev. Biol., 266, 43–61, doi:10.1016/j.ydbio.2003.10.002, 2004.

Knabe, W.: Die Morphogenese der Megamitochondrien in den Zapfen von *Tupaia belangeri* (Tupaiidae, Scandentia, Mammalia), Doctoral thesis, Department of Morphology, University of Göttingen, Germany, 1995.

Knabe, W. and Kuhn, H.-J.: Morphogenesis of megamitochondria in the retinal cone inner segments of *Tupaia belangeri* (Scandentia), Cell Tissue Res., 285, 1–9, doi:10.1007/s004410050614, 1996a.

Knabe, W. and Kuhn, H.-J.: The role of microtubules and microtubule-organising centres during the migration of mitochondria, J. Anat., 189, 383–391, 1996b.

Knabe, W. and Kuhn, H.-J.: Ciliogenesis in photoreceptor cells of the tree shrew retina, Anat. Embryol., 196, 123–131, doi:10.1007/s004290050085, 1997.

Knabe, W. and Kuhn, H.-J.: Disk formation in retinal cones of *Tupaia belangeri* (Scandentia), Cell Tissue Res., 292, 67–76, doi:10.1007/s004410051035, 1998a.

Knabe, W. and Kuhn, H.-J.: Pattern of cell death during optic cup formation in the tree shrew *Tupaia belangeri*, J. Comp. Neurol., 401, 352–366, doi:10.1002/(SICI)1096-9861(19981123)401:3<352::AID-CNE4>3.0.CO;2-A, 1998b.

Knabe, W. and Kuhn, H.-J.: The earliest invasion of macrophages into the developing brain and eye of the tree shrew *Tupaia belangeri*, Anat. Embryol., 200, 393–402, doi:10.1007/s004290050288, 1999.

Knabe, W. and Kuhn, H.-J.: Capillary-contacting horizontal cells in the retina of the tree shrew *Tupaia belangeri* belong to the mammalian type A, Cell Tissue Res., 299, 307–311, doi:10.1007/s004419900151, 2000.

Knabe, W. and Ochs, M.: Horizontal cells invest retinal capillaries in the tree shrew *Tupaia belangeri*, Cell Tissue Res., 298, 33–43, doi:10.1007/s004419900072, 1999.

Knabe, W., Skatchkov, S., and Kuhn, H.-J.: "Lens mitochondria" in the retinal cones of the tree-shrew *Tupaia belangeri*, Vision Res, 37, 267–271, doi:10.1016/S0042-6989(96)00199-X, 1997.

Knabe, W., Süss, M., and Kuhn, H.-J.: The patterns of cell death and of macrophages in the developing forebrain of the tree shrew *Tupaia belangeri*, Anat. Embryol., 201, 157–168, doi:10.1007/PL00008237, 2000.

Knabe, W., Washausen, S., Brunnett, G., and Kuhn, H.-J.: Use of "reference series" to realign histological serial sections for three-dimensional reconstructions of the positions of cellular events in the developing brain, J. Neurosci. Methods, 121, 169–180, doi:10.1016/S0165-0270(02)00247-9, 2002.

Knabe, W., Knerlich, F., Washausen, S., Kietzmann, T., Sirén, A. L., Brunnett, G., Kuhn, H.-J., and Ehrenreich, H.: Expression patterns of erythropoietin and its receptor in the developing mid-

brain, Anat. Embryol., 207, 503–512, doi:10.1007/s00429-003-0365-y, 2004a.

Knabe, W., Washausen, S., Brunnett, G., and Kuhn, H.-J.: Rhombomere-specific patterns of apoptosis in the tree shrew *Tupaia belangeri*, Cell Tissue Res., 316, 1–13, doi:10.1007/s00441-004-0855-0, 2004b.

Knabe, W., Washausen, S., Happel, N., and Kuhn, H.-J.: Development of starburst cholinergic amacrine cells in the retina of *Tupaia belangeri*, J. Comp. Neurol., 502, 584–597, doi:10.1002/cne.21324, 2007.

Knabe, W., Washausen, S., Happel, N., and Kuhn, H.-J.: Diversity in mammalian chiasmatic architecture: Ipsilateral axons are deflected at glial arches in the prechiasmatic optic nerve of the eutherian *Tupaia belangeri*, J. Comp. Neurol., 508, 437–457, doi:10.1002/cne.21694, 2008.

Knabe, W., Obermayer, B., Kuhn, H.-J., Brunnett, G., and Washausen, S.: Apoptosis and proliferation in the trigeminal placode, Brain Struct. Funct., 214, 49–65, doi:10.1007/s00429-009-0228-2, 2009.

Kong, S., Du, X., Peng, C., Wu, Y., Li, H., Jin, X., Hou, L., Deng, K., Xu, T., and Tao, W.: Dlic1 deficiency impairs ciliogenesis of photoreceptors by destabilizing dynein, Cell Res., 23, 835–850, doi:10.1038/cr.2013.59, 2013.

Köpsel, H.-J.: Die Tuba uterina von *Tupaia belangeri*. Makroskopische und mikroskopische Anatomie. Veränderungen während der Gravidität, Doctoral thesis, Department of Morphology, University of Göttingen, Germany, 1988.

Kosaka, K. and Kosaka, T.: Organization of the main olfactory bulbs of some mammals: Musk shrews, moles, hedgehogs, tree shrews, bats, mice, and rats, J. Comp. Neurol., 472, 1–12, doi:10.1002/cne.20004, 2004.

Kriesell, W.: Das Ovar von Tupaia, Doctoral thesis, Department of Morphology, University of Göttingen, Germany, 1977.

Kühne, J.-H.: Rod receptors in the retina of *Tupaia belangeri*, Anat. Embryol., 167, 95–102, doi:10.1007/BF00304603, 1983.

Kuhn, H.-J. and Liebherr, G.: The early development of the heart of *Tupaia belangeri*, with reference to other mammals., Anat. Embryol., 176, 53–63, doi:10.1007/BF00309752, 1987.

Kuhn, H.-J. and Liebherr, G.: The early development of the epicardium in *Tupaia belangeri*, Anatomy and Embryology, 177, 225–234, doi:10.1007/BF00321133, 1988.

Kuhn, H.-J. and Schwaier, A.: Implantation, early placentation, and the chronology of embryogenesis in *Tupaia belangeri*, Z. Anat. Entwicklungsgesch., 142, 315–340, doi:10.1007/BF00519135, 1973.

Kuhn, H.-J. and Starck, D.: Die Tupaia-Zucht des Dr. Senckenbergischen Anatomischen Institutes, Nat. Mus., 96, 263–271, 1966.

Kunz, Y. W. and Regan, C.: Histochemical investigations into the lipid nature of the oil-droplet in the retinal twin-cones of *Lebistes reticulatus* (Peters), Rev. Suisse Zool., 80, 699–703, 1973.

Kunz, Y. W. and Wise, C.: Structural differences of cone "oil-droplets" in the light and dark adapted retina of *Poecilia reticulata* P., Experientia, 34, 246–249, doi:10.1007/BF01944706, 1978.

Kurz, H., Korn, J., Eggli, P. S., Huang, R., and Christ, B.: Embryonic central nervous system angiogenesis does not involve blood-borne endothelial progenitors, J. Comp. Neurol., 436, 263–274, doi:10.1002/cne.1066, 2001.

Larsell, O.: The nervus terminalis, Ann. Otol. Rhinol. Laryngol., 59, 414–438, doi:10.1177/000348945005900211, 1950.

Lee, V. M., Sechrist, J. W., Luetolf, S., and Bronner-Fraser, M.: Both neural crest and placode contribute to the ciliary ganglion and oculomotor nerve, Dev. Biol., 263, 176–190, doi:10.1016/j.ydbio.2003.07.004, 2003.

Levi, G., Puche, A. C., Mantero, S., Barbieri, O., Trombino, S., Paleari, L., Egeo, A., and Merlo, G. R.: The *Dlx5* homeodomain gene is essential for olfactory development and connectivity in the mouse, Mol. Cell. Neurosci., 22, 530–543, doi:10.1016/S1044-7431(02)00041-6, 2003.

Li, Y., Liu, T., Duan, W., Song, X., Shi, G., Zhang, J., Deng, X., Zhang, S., and Hou, X.: Instability in mitochondrial membranes in Polima cytoplasmic male sterility of *Brassica rapa* ssp. *chinensis*, Funct. Integr. Genomics, 14, 441–451, doi:10.1007/s10142-014-0368-1, 2014.

Liebherr, G.: Die Ontogenese des Venensystems der Leber von *Tupaia belangeri* (Tupaiidae, Scandentia, Mammalia), Doctoral thesis, Department of Morphology, University of Göttingen, Germany, 1983.

Liu, C. H., Wang, I. J., Wei, F. D., and Chien, C. L.: Neuronal intermediate filament α-internexin is expressed by neuronal lineages in the developing chicken retina, Exp. Eye Res., 110, 18–25, doi:10.1016/j.exer.2013.02.013, 2013.

Lluch, S., López-Fuster, M. J., and Ventura, J.: Giant mitochondria in the retina cone inner segments of shrews of genus *Sorex* (Insectivora, Soricidae), Anat. Rec. A Discov. Mol. Cell Evol. Biol., 272, 484–490, doi:10.1002/ar.a.10066, 2003.

Lluch, S., López-Fuster, M. J., and Ventura, J.: Cornea, retina, and lens morphology in five Soricidae species (Soricomorpha: Mammalia), Anat. Sci. Int., 84, 312–322, doi:10.1007/s12565-009-0042-1, 2009.

Lumsden, A. and Keynes, R.: Segmental patterns of neuronal development in the chick hindbrain, Nature, 337, 424–428, doi:10.1038/337424a0, 1989.

Lumsden, A., Sprawson, N., and Graham, A.: Segmental origin and migration of neural crest cells in the hindbrain region of the chick embryo, Development, 113, 1281–1291, 1991.

Ma, B., Lin, Z., Winkelbach, S., Lindenmaier, W., and Dittmar, K. E.: Automatic registration of serial sections of mouse lymph node by using Image-Reg, Micron, 39, 387–396, doi:10.1016/j.micron.2007.03.005, 2008a.

Ma, B., Wang, L., von Wasielewski, R., Lindenmaier, W., and Dittmar, K. E.: Serial sectioning and three-dimensional reconstruction of mouse Peyer's patch, Micron, 39, 967–975, doi:10.1016/j.micron.2007.10.007, 2008b.

Maas, J.-H.: Die Morphogenese des Sinus venosus von *Tupaia belangeri*, Diploma thesis, Department of Morphology, University of Göttingen, Germany, 1992.

MacLaren, R. E.: A glial palisade delineates the ipsilateral optic projection in *Monodelphis*, Vis. Neurosci., 15, 397–400, 1998.

MacNichol Jr., E. F., Kunz, Y. W., Levine, J. S., Hárosi, F. I., and Collins, B. A.: Ellipsosomes: Organelles containing a cytochrome-like pigment in the retinal cones of certain fishes, Science, 200, 549–552, doi:10.1126/science.644317, 1978.

Malz, C. R. and Kuhn, H.-J.: FMRFamide immunoreactivity and the invasion of adenohypophyseal cells into the neural lobe in the developing pituitary of the tree shrew *Tupaia belangeri*, Brain Res, 834, 83–88, doi:10.1016/S0006-8993(99)01555-3, 1999.

Malz, C. R. and Kuhn, H.-J.: Calretinin and FMRFamide immunoreactivity in the nervus terminalis of prenatal tree shrews (*Tupaia belangeri*), Brain Res. Dev. Brain Res., 135, 39–44, doi:10.1016/S0165-3806(02)00299-7, 2002.

Malz, C. R., Schwartz, P., and Kuhn, H.-J.: Lectin binding sites in the vomeronasal organ and the olfactory epithelium of the tree shrew *Tupaia belangeri*, J. Hirnforsch., 39, 481–487, 1999.

Malz, C. R., Knabe, W., and Kuhn, H.-J.: Pattern of calretinin immunoreactivity in the main olfactory system and the vomeronasal system of the tree shrew, *Tupaia belangeri*, J. Comp. Neurol., 420, 428–436, doi:10.1002/(SICI)1096-9861(20000515)420:4<428::AID-CNE2>3.0.CO;2-2, 2000.

Malz, C. R., Knabe, W., and Kuhn, H.-J.: Calretinin immunoreactivity in the prenatally developing olfactory systems of the tree shrew *Tupaia belangeri*, Anat. Embryol., 205, 83–97, doi:10.1007/s00429-002-0244-y, 2002.

Marzban, H., Chung, S. H., Pezhouh, M. K., Feirabend, H., Watanabe, M., Voogd, J., and Hawkes, R.: Antigenic compartmentation of the cerebellar cortex in the chicken (*Gallus domesticus*), J. Comp. Neurol., 518, 2221–2239, doi:10.1002/cne.22328, 2010.

Marzban, H. and Hawkes, R.: On the architecture of the posterior zone of the cerebellum, Cerebellum, 10, 422–434, doi:10.1007/s12311-010-0208-3, 2011.

Marzban, H., Hoy, N., Marotte, L. R., and Hawkes, R.: Antigenic compartmentation of the cerebellar cortex in an Australian marsupial, the tammar wallaby *Macropus eugenii*, Brain. Behav. Evol., 80, 196–209, doi:10.1159/000340069, 2012.

Matsumoto, S., Kuhn, H.-J., Vogt, B., and Gerke, M.: Embryological development of the arterial system of the forelimb in Tupaia, Anat. Rec., 240, 416–422, doi:10.1002/ar.1092400314, 1994.

McIntyre, P. and Pask, C.: The Stiles–Crawford effect: A theoretical revisit, J. Mod. Opt., 60, 266–283, doi:10.1080/09500340.2013.770575, 2013.

Mojumder, D. K.: Capillary-contacting horizontal cells in the rodent retina, J. Anat. Soc. India, 57, 34–36, 2008.

Morona, R. and González, A.: Calbindin-D28k and calretinin expression in the forebrain of anuran and urodele amphibians: Further support for newly identified subdivisions, J. Comp. Neurol., 511, 187–220, doi:10.1002/cne.21832, 2008.

Morona, R., López, J. M., and González, A.: Localization of calbindin-D28k and calretinin in the brain of *Dermophis mexicanus* (amphibia: gymnophiona) and its bearing on the interpretation of newly recognized neuroanatomical regions, Brain Behav. Evol., 77, 231–269, doi:10.1159/000329521, 2011.

Müller, F. and O'Rahilly, R.: The initial appearance of the cranial nerves and related neuronal migration in staged human embryos, Cells Tissues Organs, 193, 215–238, 10.1159/000320026, 2011.

Müller, B. and Peichl, L.: Topography of cones and rods in the tree shrew retina, J. Comp. Neurol., 282, 581–594, doi:10.1002/cne.902820409, 1989.

Müller, B. and Peichl, L.: Morphology and distribution of catecholaminergic amacrine cells in the cone-dominated tree shrew retina, J. Comp. Neurol., 308, 91–102, doi:10.1002/cne.903080109, 1991a.

Müller, B. and Peichl, L.: Rod bipolar cells in the cone-dominated retina of the tree shrew *Tupaia belangeri*, Vis. Neurosci., 6, 629–639, doi:10.1017/S0952523800002625, 1991b.

Navascués, J., Martín-Partido, G., Alvarez, I. S., and Rodríguez-Gallardo, L.: Cell death in suboptic necrotic centers of chick embryo diencephalon and their topographic relationship with the earliest optic fiber fascicles, J. Comp. Neurol., 278, 34–46, doi:10.1002/cne.902780103, 1988.

Neveu, M. M., Holder, G. E., Ragge, N. K., Sloper, J. J., Collin, J. R., and Jeffery, G.: Early midline interactions are important in mouse optic chiasm formation but are not critical in man: A significant distinction between man and mouse, Eur. J. Neurosci., 23, 3034–3042, doi:10.1111/j.1460-9568.2006.04827.x, 2006.

Ni, M. M., Luo, Y., Liu, J., Liao, D. Q., and Tang, Y. D.: FMRFamide modulates outward potassium currents in mouse olfactory sensory neurons, Clin. Exp. Pharmacol. Physiol., 35, 563–567, doi:10.1111/j.1440-1681.2007.04840.x, 2008.

Nie, W., Fu, B., O'Brien, P., Wang, J., Su, W., Tanomtong, A., Volobouev, V., Ferguson-Smith, M., and Yang, F.: Flying lemurs – The "flying tree shrews"? Molecular cytogenetic evidence for a Scandentia-Dermoptera sister clade, BMC Biol., 6, doi:10.1186/1741-7007-6-18, 2008.

Obata, S. and Usukura, J.: Morphogenesis of the photoreceptor outer segment during postnatal development in the mouse (BALB/c) retina, Cell Tissue Res., 269, 39–48, doi:10.1007/BF00384724, 1992.

Obermayer, B.: Muster und Funktionen von Apoptose und Proliferation während der Morphogenese der Trigeminusplakode von *Tupaia belangeri* (Tupaiidae, Scandentia, Mammalia), Doctoral thesis, Department of Anatomy and Embryology, University of Göttingen, Germany, 2009.

Ochs, M., Mayhew, T. M., and Knabe, W.: To what extent are the retinal capillaries ensheathed by Müller cells? A stereological study in the tree shrew *Tupaia belangeri*, J. Anat., 196, 453–461, doi:10.1046/j.1469-7580.2000.19630453.x, 2000.

Otte, V.: Die Ausbreitung des Epikards bei *Tupaia belangeri* (Tupaiidae, Scandentia, Mammalia), Doctoral thesis, Department of Morphology, University of Göttingen, Germany, 1991.

Pakan, J. M., Iwaniuk, A. N., Wylie, D. R., Hawkes, R., and Marzban, H.: Purkinje cell compartmentation as revealed by zebrin II expression in the cerebellar cortex of pigeons (*Columba livia*), J. Comp. Neurol., 501, 619–630, doi:10.1002/cne.21266, 2007.

Park, D., Zawacki, S. R., and Eisthen, H. L.: Olfactory signal modulation by molluscan cardioexcitatory tetrapeptide (FMRFamide) in axolotls (*Ambystoma mexicanum*), Chem. Senses, 28, 339–348, doi:10.1093/chemse/28.4.339, 2003a.

Park, S. H., Park, J. W., Park, S. J., Kim, K. Y., Chung, J. W., Chun, M. H., and Oh, S. J.: Apoptotic death of photoreceptors in the streptozotocin-induced diabetic rat retina, Diabetologia, 46, 1260–1268, doi:10.1007/s00125-003-1177-6, 2003b.

Pearring, J. N., Salinas, R. Y., Baker, S. A., and Arshavsky, V. Y.: Protein sorting, targeting and trafficking in photoreceptor cells, Prog. Retin. Eye Res., 36, 24–51, doi:10.1016/j.preteyeres.2013.03.002, 2013.

Pérez de Sevilla Müller, L., Shelley, J., and Weiler, R.: Displaced amacrine cells of the mouse retina, J. Comp. Neurol., 505, 177–189, doi:10.1002/cne.21487, 2007.

Petros, T. J., Rebsam, A., and Mason, C. A.: Retinal axon growth at the optic chiasm: to cross or not to cross, Annu. Rev. Neurosci., 31, 295–315, doi:10.1146/annurev.neuro.31.060407.125609, 2008.

Petry, H. M. and Hárosi, F. I.: Visual pigments of the tree shrew (*Tupaia belangeri*) and greater galago (*Galago crassicaudatus*):

A microspectrophotometric investigation, Vision Res., 30, 839–851, doi:10.1016/0042-6989(90)90053-N, 1990.

Phelan, P. E., Mellon, M. T., and Kim, C. H.: Functional characterization of full-length TLR3, IRAK-4, and TRAF6 in zebrafish (*Danio rerio*), Mol. Immunol., 42, 1057–1071, doi:10.1016/j.molimm.2004.11.005, 2005.

Pombal, M. A., de Arriba, M. C., Sampedro, C., Alvarez, R., and Megías, M.: Immunocytochemical localization of calretinin in the olfactory system of the adult lamprey, *Lampetra fluviatilis*, Brain Res. Bull., 57, 281–283, doi:10.1016/S0361-9230(01)00701-8, 2002.

Pont-Lezica, L., Béchade, C., Belarif-Cantaut, Y., Pascual, O., and Bessis, A.: Physiological roles of microglia during development, J. Neurochem., 119, 901–908, doi:10.1111/j.1471-4159.2011.07504.x, 2011.

Primmer, S. R.: In search of a model species for aging research: A study of the life span of tree shrews, J. Anti Aging Med., 5, 179–201, doi:10.1089/10945450260195621, 2002.

Radlanski, R. J. and Renz, H.: An atlas of prenatal development of the human orofacial region, Eur. J. Oral. Sci., 118, 321–324, doi:10.1111/j.1600-0722.2010.00756.x, 2010.

Ramsey, M. and Perkins, B. D.: Basal bodies exhibit polarized positioning in zebrafish cone photoreceptors, J. Comp. Neurol., 521, 1803–1816, doi:10.1002/cne.23260, 2013.

Rasmussen, S. L., Holland, L. Z., Schubert, M., Beaster-Jones, L., and Holland, N. D.: Amphioxus *AmphiDelta*: Evolution of Delta protein structure, segmentation, and neurogenesis, Genesis, 45, 113–122, doi:10.1002/dvg.20278, 2007.

Rehkämper, G.: Untersuchungen über den Neocortex von *Tupaia belangeri* unter Berücksichtigung seiner Ontogenese, Wiss. Hausarbeit für die 1. Staatsprüfung für das Lehramt an Gymnasien, Kiel, Germany, 1977.

Röll, B.: Characterization of retinal oil droplets in diurnal geckos (reptilia, gekkonidae), J. Exp. Zool., 287, 467–476, doi:10.1002/1097-010X(20001201)287:7<467::AID-JEZ2>3.0.CO;2-8, 2000.

Saint-Jeannet, J. P. and Moody, S. A.: Establishing the pre-placodal region and breaking it into placodes with distinct identities, Dev. Biol., 389, 13–27, doi:10.1016/j.ydbio.2014.02.011, 2014.

Saito, T. H., Nakane, R., Akazome, Y., Abe, H., and Oka, Y.: Electrophysiological analysis of the inhibitory effects of FMRFamide-like peptides on the pacemaker activity of gonadotropin-releasing hormone neurons, J. Neurophysiol., 104, 3518–3529, doi:10.1152/jn.01027.2009, 2010.

Samorajski, T., Ordy, J. M., and Keefe, J. R.: Structural organization of the retina in the tree shrew (*Tupaia glis*), J. Cell. Biol., 28, 489–504, doi:10.1083/jcb.28.3.489, 1966.

Sánchez-Guardado, L., Puelles, L., and Hidalgo-Sánchez, M.: Fate map of the chicken otic placode, Development, 141, 2302–2312, doi:10.1242/dev.101667, 2014.

Sandmann, D., Engelmann, R., and Peichl, L.: Starburst cholinergic amacrine cells in the tree shrew retina, J. Comp. Neurol., 389, 161–176, doi:10.1002/(SICI)1096-9861(19971208)389:1<161::AID-CNE12>3.0.CO;2-O, 1997.

Santos, A. M., Calvente, R., Tassi, M., Carrasco, M. C., Martín-Oliva, D., Marín-Teva, J. L., Navascués, J., and Cuadros, M. A.: Embryonic and postnatal development of microglial cells in the mouse retina, J. Comp. Neurol., 506, 224–239, doi:10.1002/cne.21538, 2008.

Schleicher, A., Morosan, P., Amunts, K., and Zilles, K.: Quantitative architectural analysis: a new approach to cortical mapping, J. Autism Dev. Disord., 39, 1568–1581, doi:10.1007/s10803-009-0790-8, 2009.

Schlosser, G.: Hypobranchial placodes in *Xenopus laevis* give rise to hypobranchial ganglia, a novel type of cranial ganglia, Cell Tissue Res., 312, 21–29, doi:10.1007/s00441-003-0710-8, 2003.

Schlosser, G.: Induction and specification of cranial placodes, Dev. Biol., 294, 303–351, doi:10.1016/j.ydbio.2006.03.009, 2006.

Schlosser, G.: Making senses: Development of vertebrate cranial placodes, Int. Rev. Cell. Mol. Biol., 283, 129–234, doi:10.1016/S1937-6448(10)83004-7, 2010.

Schmitz, J., Ohme, M., and Zischler, H.: The complete mitochondrial genome of *Tupaia belangeri* and the phylogenetic affiliation of Scandentia to other eutherian orders, Mol. Biol. Evol., 17, 1334–1343, 2000.

Schönemann, F. N.: Die Frühentwicklung des Myocards von *Tupaia belangeri* (Tupaiidae, Scandentia, Mammalia), Diploma thesis, Department of Morphology, University of Göttingen, Germany, 1990.

Schumann, S.: Die pränatale Ossifikation des postkranialen Skeletts von *Tupaia belangeri*: Ein Beitrag zur Charakterisierung von Ontogeneseabläufen, Doctoral thesis, Department of Morphology, University of Göttingen, Germany, 1984.

Schunke, A. C. and Zeller, U.: Chondrocranium and dermal bones of the Lowland Streaked Tenrec *Hemicentetes semispinosus* (Afrosoricida, Tenrecidae) and their comparison with *Potamogale* and other insectivoran-grade placental mammals, Vertebr. Zool., 60, 37–72, 2010.

Schwaier, A.: Breeding tupaias (*Tupaia belangeri*) in captivity, Z. Versuchstierkd., 15, 255–271, 1973.

Schwaier, A.: A cage for the successful maintenance of tree shrews (*Tupaia belangeri*) in captivity, Z. Versuchstierkd., 16, 337–340, 1974.

Schwaller, B.: Calretinin: From a "simple" Ca^{2+} buffer to a multifunctional protein implicated in many biological processes, Front. Neuroanat., 8, 3, doi:10.3389/fnana.2014.00003, 2014.

Sechrist, J., Nieto, M. A., Zamanian, R. T., and Bronner-Fraser, M.: Regulative response of the cranial neural tube after neural fold ablation: Spatiotemporal nature of neural crest regeneration and up-regulation of Slug, Development, 121, 4103–4115, 1995.

Shimp, K. L., Bhatnagar, K. P., Bonar, C. J., and Smith, T. D.: Ontogeny of the nasopalatine duct in primates, Anat. Rec. A Discov. Mol. Cell. Evol. Biol., 274, 862–869, doi:10.1002/ar.a.10101, 2003.

Sillitoe, R. V., Malz, C. R., Rockland, K., and Hawkes, R.: Antigenic compartmentation of the primate and tree shrew cerebellum: A common topography of zebrin II in *Macaca mulatta* and *Tupaia belangeri*, J. Anat., 204, 257–269, doi:10.1111/j.0021-8782.2004.00282.x, 2004.

Solodkin, A., Peri, E., Chen, E. E., Ben-Jacob, E., and Gomez, C. M.: Loss of intrinsic organization of cerebellar networks in spinocerebellar ataxia type 1: Correlates with disease severity and duration, Cerebellum, 10, 218–232, doi:10.1007/s12311-010-0214-5, 2011.

Solovei, I., Kreysing, M., Lanctôt, C., Kösem, S., Peichl, L., Cremer, T., Guck, J., and Joffe, B.: Nuclear architecture of rod photoreceptor cells adapts to vision in mammalian evolution, Cell, 137, 356–368, doi:10.1016/j.cell.2009.01.052, 2009.

Steinberg, R. H., Fisher, S. K., and Anderson, D. H.: Disc morphogenesis in vertebrate photoreceptors, J. Comp. Neurol., 190, 501–508, doi:10.1002/cne.901900307, 1980.

Steinecker, N.: Die frühe Ontogenese der Vena cardinalis anterior und ihrer Zuflüsse bei *Tupaia belangeri* (Tupaiidae, Scandentia, Mammalia), Doctoral thesis, Department of Morphology, University of Göttingen, Germany, 1989.

Streit, A.: The preplacodal region: An ectodermal domain with multipotential progenitors that contribute to sense organs and cranial sensory ganglia, Int. J. Dev. Biol., 51, 447–461, doi:10.1387/ijdb.072327as, 2007.

Sugihara, I. and Quy, P. N.: Identification of aldolase C compartments in the mouse cerebellar cortex by olivocerebellar labeling, J. Comp. Neurol., 500, 1076–1092, doi:10.1002/cne.21219, 2007.

Sun, S. K., Dee, C. T., Tripathi, V. B., Rengifo, A., Hirst, C. S., and Scotting, P. J.: Epibranchial and otic placodes are induced by a common Fgf signal, but their subsequent development is independent, Dev. Biol., 303, 675–686, doi:10.1016/j.ydbio.2006.12.008, 2007.

Süss, M., Knabe, W., Kuhn, H.-J., Smolej, V., and Venus, B.: Exakte Bilderfassung großer Objekte am Beispiel histologischer Schnitte, GIT Labor-Fachzeitschrift, 8, 948–949, 2000.

Süss, M., Washausen, S., Kuhn, H.-J., and Knabe, W.: High resolution scanning and three-dimensional reconstruction of cellular events in large objects during brain development, J. Neurosci. Methods, 113, 147–158, doi:10.1016/S0165-0270(01)00486-1, 2002.

Suwanpradid, J., Rojas, M., Behzadian, M. A., Caldwell, R. W., and Caldwell, R. B.: Arginase 2 deficiency prevents oxidative stress and limits hyperoxia-induced retinal vascular degeneration, PLoS One, 9, e110604, doi:10.1371/journal.pone.0110604, 2014.

Swadzba, M. E., Hauck, S. M., Naim, H. Y., Amann, B., and Deeg, C. A.: Retinal glycoprotein enrichment by concanavalin a enabled identification of novel membrane autoantigen synaptotagmin-1 in equine recurrent uveitis, PLoS One, 7, e50929, doi:10.1371/journal.pone.0050929, 2012.

Tarboush, R., Chapman, G. B., and Connaughton, V. P.: Ultrastructure of the distal retina of the adult zebrafish, *Danio rerio*, Tissue Cell, 44, 264–279, doi:10.1016/j.tice.2012.04.004, 2012.

Tarboush, R., Novales Flamarique, I., Chapman, G. B., and Connaughton, V. P.: Variability in mitochondria of zebrafish photoreceptor ellipsoids, Vis. Neurosci., 31, 11–23, doi:10.1017/S095252381300059X, 2014.

Taylor, J. S. and Guillery, R. W.: Early development of the optic chiasm in the gray short-tailed opossum, *Monodelphis domestica*, J. Comp. Neurol., 350, 109–121, doi:10.1002/cne.903500108, 1994.

Teddy, J. M. and Kulesa, P. M.: In vivo evidence for short- and long-range cell communication in cranial neural crest cells, Development, 131, 6141–6151, doi:10.1242/dev.01534, 2004.

Theveneau, E. and Mayor, R.: Neural crest migration: Interplay between chemorepellents, chemoattractants, contact inhibition, epithelial-mesenchymal transition, and collective cell migration, Wiley Interdiscip. Rev. Dev. Biol., 1, 435–445, doi:10.1002/wdev.28, 2012.

Trainor, P. A., Sobieszczuk, D., Wilkinson, D., and Krumlauf, R.: Signalling between the hindbrain and paraxial tissues dictates neural crest migration pathways, Development, 129, 433–442, 2002.

Traver, D., Herbomel, P., Patton, E. E., Murphey, R. D., Yoder, J. A., Litman, G. W., Catic, A., Amemiya, C. T., Zon, L. I., and Trede, N. S.: The zebrafish as a model organism to study development of the immune system, Adv. Immunol., 81, 253–330, doi:10.1016/S0065-2776(03)81007-6, 2003.

Usukura, J. and Obata, S.: Morphogenesis of photoreceptor outer segments in retinal development, Prog. Ret. Eye Res., 15, 113–125, doi:10.1016/1350-9462(95)00006-2, 1995.

Vilensky, J. A.: The neglected cranial nerve: nervus terminalis (cranial nerve N), Clin. Anat., 27, 46–53, doi:10.1002/ca.22130, 2014.

Wang, X., Kochetkova, I., Haddad, A., Hoyt, T., Hone, D. M., and Pascual, D. W.: Transgene vaccination using *Ulex europaeus* agglutinin I (UEA-1) for targeted mucosal immunization against HIV-1 envelope, Vaccine, 23, 3836–3842, doi:10.1016/j.vaccine.2005.02.023, 2005.

Washausen, S. and Knabe, W.: Apoptosis contributes to placode morphogenesis in the posterior placodal area of mice, Brain Struct. Funct., 218, 789–803, doi:10.1007/s00429-012-0429-y, 2013.

Washausen, S., Obermayer, B., Brunnett, G., Kuhn, H.-J., and Knabe, W.: Apoptosis and proliferation in developing, mature, and regressing epibranchial placodes, Dev. Biol., 278, 86–102, doi:10.1016/j.ydbio.2004.10.016, 2005.

Wheway, G., Parry, D. A., and Johnson, C. A.: The role of primary cilia in the development and disease of the retina, Organogenesis, 10, 69–85, doi:10.4161/org.26710, 2014.

Williams, S. E., Mason, C. A., and Herrera, E.: The optic chiasm as a midline choice point, Curr. Opin. Neurobiol., 14, 51–60, doi:10.1016/j.conb.2004.01.010, 2004.

Wirsig-Wiechmann, C. R., Wiechmann, A. F., and Eisthen, H. L.: What defines the nervus terminalis? Neurochemical, developmental, and anatomical criteria, Prog. Brain Res., 141, 45–58, doi:10.1016/S0079-6123(02)41083-7, 2002.

Wolbarsht, M. L.: The function of intraocular color filters, Fed. Proc., 35, 44–50, 1976.

Yoshida, K., Watanabe, D., Ishikane, H., Tachibana, M., Pastan, I., and Nakanishi, S.: A key role of starburst amacrine cells in originating retinal directional selectivity and optokinetic eye movement, Neuron, 30, 771–780, doi:10.1016/S0896-6273(01)00316-6, 2001.

Young, J. M., Massa, H. F., Hsu, L., and Trask, B. J.: Extreme variability among mammalian V1R gene families, Genome Res., 20, 10–18, doi:10.1101/gr.098913.109, 2010.

Zeller, U.: Zur Ontogenese und Morphologie des Craniums von *Tupaia belangeri* (Tupaiidae, Scandentia, Mammalia), Doctoral thesis, Department of Morphology, University of Göttingen, Germany, 1983.

Zeller, U. and Kuhn, H.-J.: Postpartum erythrophagocytosis, iron storage and iron secretion in the endometrium of the tree shrew (Tupaia) during pregnancy, J. Anat., 184, 597–606, 1994.

Zhang, W. and Delay, R. J.: Pulse stimulation with odors or IBMX/forskolin potentiates responses in isolated olfactory neurons, Chem. Senses, 31, 197–206, doi:10.1093/chemse/bjj017, 2006.

Zhang, P., Yang, C., and Delay, R. J.: Urine stimulation activates BK channels in mouse vomeronasal neurons, J. Neurophysiol., 100, 1824–1834, doi:10.1152/jn.90555.2008, 2008.

Zhang, J., Li, Y., Shi, G., Chen, X., Wang, J., and Hou, X.: Characterization of α-tubulin gene distinctively presented in a cytoplasmic male sterile and its maintainer line of non-heading Chinese cabbage, J. Sci. Food Agric., 89, 274–280, doi:10.1002/jsfa.3438, 2009.

Zilles, K. J.: Ontogenesis of the visual system, edited by: Brodal, A., Hild, W., van Limborgh, J., Ortmann, R., Schiebler, T. H., Töndury, G., and Wolff, E., Adv. Anat. Embryol. Cell Biol., 54, Springer, Berlin, Germany, 1978.